

Review

Preparation of Nanocellulose-Based Aerogel and Its Research Progress in Wastewater Treatment

Jiaxin Zhao ¹, Xushuo Yuan ¹, Xiaoxiao Wu ¹, Li Liu ¹, Haiyang Guo ², Kaimeng Xu ^{1,*}, Lianpeng Zhang ^{1,*} and Guanben Du ¹

¹ Yunnan Provincial Key Laboratory of Wood Adhesives and Glued Products, Southwest Forestry University, Kunming 650224, China

² Jiaying Key Laboratory of Molecular Recognition and Sensing, College of Biological, Chemical Sciences and Engineering, Jiaying University, Jiaying 314001, China

* Correspondence: xukm007@163.com (K.X.); lpz@zju.edu.cn (L.Z.)

Abstract: Nowadays, the fast expansion of the economy and industry results in a considerable volume of wastewater being released, severely affecting water quality and the environment. It has a significant influence on the biological environment, both terrestrial and aquatic plant and animal life, and human health. Therefore, wastewater treatment is a global issue of great concern. Nanocellulose's hydrophilicity, easy surface modification, rich functional groups, and biocompatibility make it a candidate material for the preparation of aerogels. The third generation of aerogel is a nanocellulose-based aerogel. It has unique advantages such as a high specific surface area, a three-dimensional structure, is biodegradable, has a low density, has high porosity, and is renewable. It has the opportunity to replace traditional adsorbents (activated carbon, activated zeolite, etc.). This paper reviews the fabrication of nanocellulose-based aerogels. The preparation process is divided into four main steps: the preparation of nanocellulose, gelation of nanocellulose, solvent replacement of nanocellulose wet gel, and drying of nanocellulose wet aerogel. Furthermore, the research progress of the application of nanocellulose-based aerogels in the adsorption of dyes, heavy metal ions, antibiotics, organic solvents, and oil-water separation is reviewed. Finally, the development prospects and future challenges of nanocellulose-based aerogels are discussed.

Keywords: aerogel; nanocellulose; adsorption; wastewater treatment; application



Citation: Zhao, J.; Yuan, X.; Wu, X.; Liu, L.; Guo, H.; Xu, K.; Zhang, L.; Du, G. Preparation of Nanocellulose-Based Aerogel and Its Research Progress in Wastewater Treatment. *Molecules* **2023**, *28*, 3541. <https://doi.org/10.3390/molecules28083541>

Academic Editors: Xiaolong Ji and Xin Wang

Received: 22 March 2023

Revised: 12 April 2023

Accepted: 14 April 2023

Published: 17 April 2023



Copyright: © 2023 by the authors. Licensee MDPI, Basel, Switzerland. This article is an open access article distributed under the terms and conditions of the Creative Commons Attribution (CC BY) license (<https://creativecommons.org/licenses/by/4.0/>).

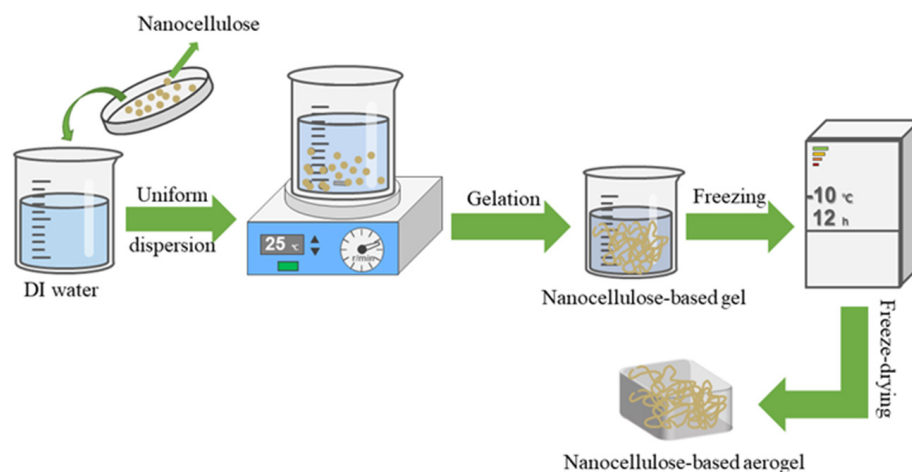
1. Introduction

Among the most fundamental requirements for survival, water is absolutely crucial for all forms of life on Earth. However, the rapid growth of the world population, the construction of modern cities, and the development of industrialization have led to the pollution of a large amount of water quality environment. This issue has been an ongoing global problem. Therefore, water environment management has become one of the most critical parts of global environmental governance [1,2]. Due to various industrial and human activities, there is a large amount of harmful substances in wastewater. It mainly includes dyes, heavy metal ions, petroleum, organic solvents, and antibiotics. The long-term accumulation of these harmful substances in nature can cause serious complications for humans and animals and cause serious damage to the environment [3,4]. Therefore, it is necessary to eliminate these harmful substances before discharging wastewater to reduce their contaminating effects on earthly organisms and the environment. Reverse osmosis, ion exchange, chemical precipitation, filtration, solvent extraction, oxidation, coagulation, and adsorption are common methods for removing hazardous substances from wastewater [5,6]. In these technologies, the main principle of adsorption is the interaction between the contaminant and the adsorbent, which causes the contaminant to be immobilized on the surface of the adsorbent by the interaction. They primarily comprise electrostatic interactions, hydrogen bonding, ion exchange, van der Waals forces, and hydrophobic interactions [7]. In addition, adsorption technology has many advantages,

such as eco-friendliness, low processing costs, and the availability of large quantities of materials for use as adsorbents [3]. Therefore, adsorption technology is considered to be one of the simplest and easiest to operate and implement [8]. Due to these characteristics, adsorption technology is used extensively for wastewater remediation.

In wastewater treatment, various adsorbents are made in large quantities. For example, activated carbon, graphene, nanocellulose, metal organic skeletons, etc. In addition to the above-mentioned adsorbents, aerogels are also considered excellent candidates for adsorbents in water purification. It is an ultra-lightweight, highly porous solid material. It has a three-dimensional structure, a low density, a large specific surface area, a high porosity, and excellent vibration damping properties [9–11]. Kistler [12] created the first aerogel in the early 1930s by supercritically drying the wet gel to eliminate the liquid. In the following decades, different kinds of aerogels were made by researchers, such as inorganic aerogels [13], polymer-based aerogels [14], and nanocellulose-based aerogels [15]. Compared with organic aerogels, inorganic aerogels have obvious disadvantages, such as weak mechanical strength and fragility [15]. Nanocellulose-based aerogel has become the leading environmental material with the advantages of being green, renewable, biodegradable, etc. It is widely used in the fields of adsorbent material, catalyst carrier, filter material, heat insulation material, etc. [16,17]. Therefore, nanocellulose-based aerogels have received a lot of attention from researchers in various countries.

This paper first introduces the preparation of nanocellulose as well as nanocellulose-based aerogel. Scheme 1 shows a simple process for the preparation of nanocellulose-based aerogels. Then, the paper reviewed the recent research progress of nanocellulose aerogel in various applications such as dyes, heavy metal ions, antibiotics, organic solvents, and oil-water separation. Lastly, recommendations for future research, which explore its challenges and shortcomings and provide strategies for future study. To further extend the application of nanocellulose-based aerogel in wastewater environment treatment.



Scheme 1. A simple preparation process for nanocellulose-based aerogels.

2. Preparation of a Nanocellulose-Based Aerogel

Nanocellulose-based aerogel is the latest generation of aerogel made of nanocellulose. It not only retains the same qualities as traditional aerogel, but it also has the attributes of being renewable, green, non-toxic, low-cost, and biodegradable nanocellulose [18]. Usually, nanocellulose aerogels are prepared in four steps: preparation of the nanocellulose, gelation of the nanocellulose, solvent replacement of the nanocellulose wet gel, and drying of the nanocellulose wet gel. The structure and characteristics of nanocellulose-based aerogels are affected by each preparation process. The microstructure and characteristics of nanocellulose aerogels are also affected by different cellulose sources and production methods.

2.1. Preparation of Nanocellulose

Cellulose is the most prevalent and extensively dispersed natural polymer in nature. It is constituted of D-glucopyranose units connected by 1,4 glycosidic linkages [19,20]. Nanocellulose is a natural cellulose with a one-dimensional nanoscale size. There are three types of nanocellulose: cellulose nanocrystals (CNC), cellulose nanofilaments (CNF), and bacterial cellulose (BC) [21–23]. Table 1 shows the classification of nanocellulose. They differ in size, morphology, and preparation methods [24]. Nanocellulose offers several benefits, including a large specific surface area, biodegradability, renewable energy, and a high aspect ratio [25–27]. Nanocellulose is an important substrate in the production of nanocellulose-based aerogels. The different sources of its preparation methods and the quality of its preparation will directly affect the performance and application of nanocellulose-based aerogels.

Table 1. Classification of nanocellulose.

Category	Source	Preparation Method	Advantages	Disadvantages	Ref.
Cellulose nanocrystals (CNC)	Cellulose	Acid hydrolysis High-shear mechanical stripping	High specific surface area High mechanical properties Biodegradable	Higher production costs Easy to gather	[28]
Cellulose nanofilaments (CNF)	Cellulose	Acid hydrolysis High-shear mechanical stripping Biological preparation chemical oxidative stripping	High specific surface area High mechanical properties Biodegradable Can be prepared into a variety of forms	Higher production costs Easy to gather	[29]
Bacterial cellulose (BC)	Natural cellulose material synthesized by microbial growth	Extraction from cultures by chemical and physical methods	Biodegradable Can be prepared in a variety of forms	Higher production cost Poorer mechanical properties	[30]

The common preparation methods of nanocellulose are chemical, mechanical, chemical-mechanical, and bio-enzymatic [31]. Table 2 describes the classification of nanocellulose preparation methods. The chemical method commonly used is 2,2,6,6-tetramethylpiperidin-1-yloxy (TEMPO) oxidation of cellulose. Xue et al. [32] prepared CNF by oxidizing cellulose pulp at pH = 10 using the TEMPO/NaBr/NaClO system. CNF has a high specific surface area and a consistent and concentrated pore size distribution of 10–15 nm. Chen et al. [33] prepared nanocellulose from bamboo, cotton lint, and sisal using TEMPO, NaBr, and NaClO solutions with crystallinities of 60.1%, 66.5%, and 83.9%, respectively. The widths of all three samples were in the range of 5–14 nm and showed well-dispersed forms. Wen et al. [34] prepared highly thermally stable and hydrophobic lignocellulosic nanoprimer fibers from poplar high-yield pulp by controlling different amounts of NaClO using the TEMPO oxidation system. Sun et al. [35] utilized the TEMPO oxidation system to effectively manufacture cellulose nanocrystals from bleached wood pulp. The average length is 200.7 nm, the average diameter is 5.8 nm, and the aspect ratio is 34.4. However, the TEMPO oxidation technique necessitates more stringent pH control of the reaction fluid [36]. In addition, the TEMPO oxidation procedure may result in the existence of trace levels of radical species in the sample, which may restrict the material's utility [37].

Table 2. Classification of nanocellulose preparation methods.

Preparation Method	Advantages	Disadvantages	Ref.
Mechanical preparation	Simple operation No chemical reagents are required	Limited production capacity Requiring high energy consumption equipment	[38]
Chemical preparation	Can precisely control the structure and morphology of the product	The use of chemical reagents is harmful to the human body High environmental impact	[39]

Table 2. Cont.

Preparation Method	Advantages	Disadvantages	Ref.
Bio-enzyme preparation	The production process is environmentally friendly The prepared nanocellulose has a uniform structure High cellulose decomposition rate	Enzyme preparations are expensive Take a long time to prepare	[40,41]
Acid hydrolysis preparation	Low cost Simple and easy to use stable and controllable Quality of finished products	Production environment with acidic wastewater discharge easy to produce by-products Need to treat wastewater and waste acid	[42,43]
TEMPO oxidation method preparation	The production process is environmentally friendly The prepared nanocellulose has a uniform structure High cellulose decomposition rate	TEMPO reagents are expensive Take a long time to prepare	[44]

Mechanical methods mainly use high cutting forces to break down the fiber, such as the ball milling method, the high pressure homogenization method, the ultrasonic method, etc. [45]. Although the mechanical method is less polluting to the environment, it consumes more energy, and the uniformity of the prepared nanocellulose (CNF) is poor [46]. Nevertheless, using chemical pretreatment followed by mechanical treatment can minimize mechanical treatment energy consumption while improving CNF quality. Common methods of chemical pretreatment include amine functionalization [47], carboxymethylation [48], phosphorylation [49], acetylation [50], nitration [51], etc. Chemical pretreatment creates new functional groups on the fiber surface, further broadening the application of CNF. Henschen et al. [52] prepared oxalic acid cellulose using paper pulp and oxalic acid dihydrate. Nanocellulose was then produced by high-pressure homogenization. The length and breadth of the produced nanocellulose averaged 350 nm and 3–4 nm, respectively. The bio-enzymatic method is an enzymatic treatment of fibers, and enzymatic treatment is considered a green and sustainable method for CNF preparation. Zhang et al. [53] generated nanocellulose by bio-enzymatic-assisted ultrasonication after pretreating poplar wood with the steam blasting method. The widths were in the range of 20–50 nm. They featured high aspect ratios and network entanglement structures. Tao et al. [54] used xylanase to pretreat sugarcane bagasse pulp and combined it with a mechanical method to prepare cellulose nanogenic fibers (CNF). The research revealed that the thermal stability of CNF produced after enzyme treatment increased with crystallinity. Nie et al. [55] prepared CNF suspensions with higher crystallinity by pretreating unbleached eucalyptus pulp with xylanase combined with high-pressure homogenization. It has higher dispersibility and rheology.

Acid hydrolysis is a typical process for preparing CNC. That is, the acid is utilized to break down the amorphous area of cellulose while retaining the crystalline region. This method can prepare CNC with high crystallinity, etc. The acid hydrolysis preparation process has been very well developed and industrialized into production, but the acid hydrolysis method requires high equipment materials. Kassab et al. [56] first extracted purified cellulose microfibrils (CMF) from *Juncus* plant stems by chemical methods. Sulfated cellulose nanocrystals (S-CNC) were then synthesized using the acid hydrolysis of sulfuric acid and a citric/hydrochloric acid combination. The diameter of the S-CNC is 7.3 ± 2.2 nm, the length is 431 ± 94 nm, and the crystallinity is 81%. Rashaad et al. [57] used acid hydrolysis of bamboo fibers and isolated needle-like CNC with 86.96% crystallinity from the bamboo fibers. The CNC yield rate is around 22%. BC is a naturally occurring nanostructured polymeric substance that is mostly manufactured by bacteria. Other polymers like lignin, hemicellulose, and pectin are not present in BC [58,59]. The

performance of BC is determined by the medium composition and the type of bacteria utilized [45]. Salari et al. [60] obtained xyloglucan bacilli in beet molasses, cheese whey, and standard Hestrin-Schramm (HS) medium, thereby producing BC. They prepared bacterial cellulose nanocrystals (BCNC) from the resulting BC by hydrolyzing it with sulfuric acid. The diameter and length of BCNC were 25 ± 5 nm and 306 ± 112 nm, respectively. Xu et al. [61] used sweet potato residue (SPR) hydrolysate as a medium, and the SPR hydrolysate was used directly with little to no inhibitors, which facilitated the subsequent synthesis of SPR-BC. SPR-BC has a crystallinity of 87.39% and a maximum thermal degradation temperature of 263 °C. Superior to the synthetic media preparation of BC.

2.2. Gelation of Nanocellulose

Nanocellulose gelation is a vital process for the creation of nanocellulose-based aerogels. Nanocellulose forms three-dimensional network structures during gel formation, and these network structures increase the strength of the gel. Physical cross-linking and chemical cross-linking are the two mechanisms by which gelation is formed [62]. Physical cross-linking is typically caused by inter- or intramolecular hydrogen bonding as well as physical inter-molecular entanglement. To develop a network structure, chemical cross-linking typically requires the addition of additional cross-linking agents. In general, physical cross-linking produces a less stable structure than chemical cross-linking [63]. The physical gelation system of nanocellulose is primarily dependent on the creation of intermolecular as well as intramolecular hydrogen bonds with the hydroxyl groups present on the surface of nanocellulose. Usually, the prepared nanocellulose is uniformly dispersed in water and then spontaneously forms into a hydrogel under hydrogen bonding [64]. Xing et al. [65] obtained nanocellulose from durian peel. At a concentration greater than 0.5%, it may spontaneously cross-link at room temperature to produce a hydrogel. The experimental results show that CNF aerogels containing 1% CNF exhibit a sheet-like structure supported by fibers. CNF aerogel has the highest compression ability and is 99% pore size. Shaheed et al. [66] isolated cellulose from peanut shells and then formed the gel spontaneously by high-intensity ultrasound. Pure nanocellulose aerogels (NFC aerogels) were synthesized by solvent substitution and freeze-drying. Then Cu-BTC/NFC aerogels were prepared by adding a metal-organic backbone (Cu-BTC) to the nanocellulose gels through the direct mixing method. The procedure for preparation is depicted in Figure 1. Heath et al. [67] dispersed nanocellulose in water using an aqueous-phase dispersion method, allowing spontaneous gel formation. Then, the nanocellulose-based aerogel with a density of 78 mg/cm^3 and a specific surface area of $605 \text{ m}^2/\text{g}$ was prepared by the solvent replacement technique and the supercritical CO_2 drying method. The chemical cross-linking of nanocellulose gelation happens mostly during the sol-gel technique's preparation. Zhu et al. [68] synthesized two distinct aerogels from CNCs and CNFs using the sol-gel technique. According to the findings, at 85% strain, CNCs and CNFs aerogels had compressive strengths of 269.5 kPa and 299.5 kPa, respectively. Gupta et al. [69] prepared aerogels based on nano-protofibrillated cellulose and polymethylsilsesquioxane using the sol-gel method. A sol-gel preparation of aerogels can increase their mechanical characteristics and thermal stability and have a unique 3D network of interconnected nanoscale particles [70]. Unfortunately, the sol-gel process for preparing aerogels is time-consuming. So the rate of gelation is accelerated by adding chemical cross-linking agents to the liquid sol or by changing the physical conditions (temperature, pH, ultrasonic treatment, etc.) [71]. Mu et al. [72] designed and synthesized polyorganosiloxanes containing polyorganosiloxanes by free radical polymerization. The polyorganosiloxanes could be covalently cross-linked with cellulose nanofibers (CNF). The resulting aerogels had a 3D structure with a high specific surface area of $53.88 \text{ m}^2/\text{g}$. Ruan et al. [73] used calcium chloride as a green cross-linking agent for cellulose nanocrystals (CNC). Then freeze-dry the CNC gels. A CNC aerogel with good stability and ultra-light performance (density of 0.036 g/cm^3) was successfully prepared.

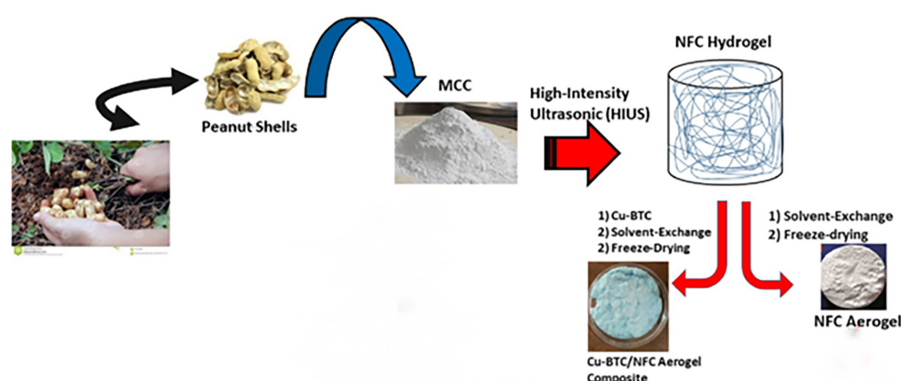


Figure 1. Synthesis of pure NFC aerogel and Cu-BTC/NFC aerogel [66] by Nuhaa Shaheed, used under CCBY4.0/Cropped from original.

2.3. Solvent Substitution of Nanocellulose Wet Gel

Solvent replacement is the process of replacing organic solvents with water in a wet gel system. It prevents the gel skeleton from collapsing during the drying process [74]. The selection of a suitable organic solvent is the most important part of the solvent replacement process. If the chosen organic solvent is destructive to the structure of the nanocellulose hydrogel itself, then the structure and characteristics of the nanocellulose aerogel will be affected. Generally, organic solvents with a lower surface tension than that of water, such as ethanol, *tert*-butanol, and acetone, are used. These organic solvents can effectively reduce the capillary pressure inside the pore and protect the pore structure of aerogel [75]. In addition, the selection of a suitable organic solvent needs to be combined with the drying method. Aerogels prepared by the freeze-drying method are usually selected with *tert*-butyl alcohol. Ethanol and acetone are frequently used in the preparation of supercritical CO₂-drying aerogels. Aerogel prepared by the atmospheric pressure drying method uses acetone, which is normally selected. Wu et al. [76] prepared biosynthesis, *tert*-butyl alcohol solvent replacement, and atom transfer radical polymerization to make functionalized biomass-derived bacterial cellulose aerogels with nano-network structure and high porosity. Zhang et al. [77] prepared CNC aerogels using different concentrations of *tert*-butanol solvent substitution and freeze-drying. Li et al. [75] prepared cellulose nanofibril-based aerogels using the acetone solvent replacement approach and atmospheric pressure drying. The results showed that the specific surface area of the prepared aerogel was 22.4 m²/g and the density was 58.82 mg/cm³. Ciftci et al. [78] prepared CNF-based hydrogels from cellulose nanofibers (CNFs) by ultrasonication, using ethanol as a replacement solvent. Then CNF aerogels were produced by drying with supercritical CO₂. The aerogel was discovered to have a low density (0.009–0.05 g/cm³), high porosity (99%), and a high surface area (72–115 m²/g).

2.4. Drying of Nanocellulose Wet Gel

Drying is the final and most crucial stage in the production of nanocellulose-based aerogels. Owing to the high number of micropores present in wet gels. When utilizing conventional drying techniques, the bending of the gas-liquid interface could cause capillary pressure, which could cause the gel pores to collapse and break. However, the supercritical CO₂ drying method and the freeze-drying method can prevent this phenomenon [63]. Thus, these two drying methods are routinely utilized to make nanocellulose-based aerogels. According to the different ways of freezing, the freeze-drying method can be divided into liquid nitrogen freeze drying and refrigerator freeze drying. Li et al. [79] successfully prepared anisotropic nanofiber aerogels loaded with modified UIO-66-EDTA by liquid nitrogen-directed freeze-drying technique. The liquid nitrogen-directed freeze-drying process is shown in Figure 2. Wu et al. [80] prepared aerogels with porous honeycomb structures from nanocellulose sols of poplar wool fibers (PCF). The density of this aerogel is only 0.3–0.4 mg/cm³, the porosity is greater than 99%, and the difference between the

pyrolysis temperatures is very small. Qiu et al. [81] prepared nanocellulose aerogels using different solvents and different drying techniques. The results show that the aerogels prepared by ionic liquid and freeze-drying have the structure of a fibrous network with pores that are about 200 nm in size. The aerogels made from a NaOH/urea solution and supercritical drying also have a 3D fibrous network structure, but their pore size is smaller, approximately 50 nm. Wang et al. [82] used calcium chloride solution to prepare nanocellulose aerogels by spontaneous gelation with *tert*-butanol solvent replacement and freeze-drying techniques. It has a shrinkage of 5.89%, a specific surface area of 164.9666 m²/g, and an average pore size of 10.01 nm. Yang et al. [83] obtained chemically cross-linked cellulose nanocrystals (CNCs) aerogels using a supercritical CO₂ drying method. CNCs aerogel has a density of just 5.6 mg/cm³, high porosity (99.6%), and a complete spatial network structure. Wang et al. [84] utilized supercritical CO₂ drying to create the nanocellulose-based aerogel. It had a high specific surface area of 353 m²/g, the average pore size was 8.86 nm, and the shrinkage was 4.03%. Despite the fact that the supercritical CO₂ drying method can keep an aerogel's three-dimensional structure from collapsing. However, it is costly and energy intensive, which limits its application. Currently, some studies have started to prepare nanocellulose-based aerogels by the atmospheric pressure drying method. Fu et al. [85] successfully prepared CNF-SiO₂ composite aerogels by atmospheric pressure drying at a temperature of 80 °C. Li et al. [86] obtained ultralight and porous cellulose-based aerogels using an atmospheric pressure drying method. The results of the analysis indicate that the aerogel had a porosity of over 98%, a density of 18 mg/cm³, and a specific surface area of over 30 m²/g. Zhang et al. [87] used an atmospheric pressure drying method to make graphene/cellulose nanocrystal hybrid aerogels with variable mechanical strengths. Georg et al. [88] first modified the hydrophobicity by immersing triphenylmethyl into the suspension of microcrystalline cellulose. The hydrophobic cellulose aerogel was then dried at an atmospheric pressure of 80 °C. It has a good skeletal structure. The atmospheric pressure drying method is simple and low-cost, and it can dry nanocellulose-based aerogels in large quantities. However, the process of atmospheric pressure drying method is not yet mature.

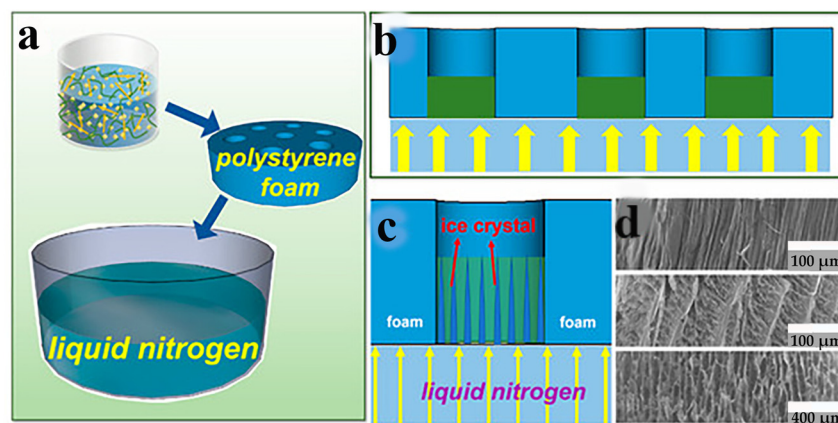


Figure 2. (a–c) A directional freeze-drying experimental procedure. (d) Morphological observation of aerogel [79] by Jiajia Li, used under CCBY/Cropped from the original.

3. Application of Nanocellulose-Based Aerogel in Wastewater Treatment

The 3D network structure of nanocellulose-based aerogels, porosity in the micro/mesoporous range, large specific surface area, surface rich in hydroxyl groups, and easy functionalization modification make them good adsorbents [89]. Table 3 briefly summarizes the properties of nanocellulose-based aerogels compared with those of other natural material-based aerogels. Presently, nanocellulose-based aerogels are effectively used to treat wastewater. Researchers have developed a number of nanocellulose-based aerogels. They can be used to adsorb dyes, heavy metal ions, antibiotics, organic solvents, and oil-water separation.

Table 3. Comparison of the properties of nanocellulose-grade aerogels with those of other natural material-based aerogels.

Aerogel Category	Source	Adjustability	Mechanical Strength	Renewability	Production Cost	Thermal Stability	Mechanical Properties	Water Resistance	Ref.
Nanocellulose-based aerogel	Cellulose	High	High	High	Low	Low	High strength High toughness	Good	[90]
Starch-based aerogel	Plant starch	Low	Low	Low	Low	Moderate	Moderate	Poor	[91]
Chitosan-based aerogel	Chitosan	High	Moderate	Moderate	Moderate	Moderate	Moderate	Good	[92]
Gelatin-based aerogel	Animal bones	Low	Moderate	Low	Moderate	Moderate	Moderate	Poor	[93]

3.1. Adsorption of Dyes

Most of the dyes in wastewater come from paper, leather, textiles, etc. They are water-soluble polymeric organic compounds with color-forming groups [94]. Dyes have a major impact on aquatic organisms. They have a significant propensity to chelate metal ions, which is hazardous to fish and other creatures and inhibits aquatic plant development [95]. Therefore, there is a global need to solve the problem of dye pollution. Recently, the use of nanocellulose-based aerogels for dye adsorption has attracted a lot of attention. Shaheed et al. [66] prepared Cu-BTC/NFC aerogel composites by compounding a metal organic backbone (Cu-BTC) with nanocellulose (NFC) using the direct mixing method. The experiments revealed that it has a good ability for adsorbing Congo red (CR). The maximal capacity for absorption is 39 mg/g. Wang et al. [96] composed a new green composite aerogel (CGS) by ultrasonically dispersing graphene oxide-silica (GO-silica) in a cellulose nanofiber suspension (CNF) and then freeze-drying the mixture. The findings showed that the composite aerogel exhibited excellent adsorption ability for methylene blue (MB) with a maximum value of 608.4 mg/g compared to the pure CNF aerogel (max = 328.3 mg/g). Xie et al. [97] prepared a high mechanical strength sodium alginate/cellulose nanofiber/polyethyleneimine composite aerogel (SCP) by combining cellulose nanofiber, sodium alginate, and polyethyleneimine. According to the results, the maximum adsorption of CR and methyl orange (MO) by SCP composite aerogel at the optimal pH (pH = 2.0–5.0) was 2007.48 mg/g and 2253.38 mg/g, respectively. Yu et al. [98] successfully synthesized composite aerogels (CNF-GnP) by assembling cellulose nanofibers (CNF) and graphene nanoplates (GnPs). It was shown that the maximum adsorption amount of CNF-GnP aerogel for CR was 585.3 mg/g, and the maximum adsorption amount for MB was 1178.5 mg/g. The binary dye absorption capacity of CNF-GnP hybrid aerogels is superior to that of pure CNF or GnP. In addition, using ethanol as a desorption agent, over 80% of CR or MB may be eluted from CNF-GnP, demonstrating the reusability of these aerogels. Maatar et al. [99] prepared cellulose aerogels based on cationic cellulose nanofibers (Q-CNF) by chemically cross-linking the nanofibers with aliphatic triisocyanates. The surface was enriched with trimethylammonium chloride functional groups. The Q-CNF aerogel was proven to be an effective adsorbent for anionic dyes and to be resistant to water disintegration. The adsorption capacities of Q-CNF for red, blue, and orange dyes were 160 mg/g, 230 mg/g, and 560 mg/g, respectively. Huo et al. [100] cross-linked CNF hydrogels by calcium ions and then immersed them in dopamine solution. Polydopamine (PDA) was used to modify the surface of CNF to produce PDA@CNF composite aerogel (PCNF). The surface area of PCNF composite aerogels is large (368.15 m²/g), and the packing density is low (27.2 mg/cm³). The experiments showed that PCNF aerogel has a strong adsorption capacity for MB. With a starting dye level of 50 mg/L, the maximum amount of MB that could be adsorbed was 208 mg/g. Grishkewich et al. [101] used dimethyl ammonium chloride (DADMAC), N,N'-methylenebis(acrylamide) (MBAA), functionalized cellulose nanofibers (CNFs), and (3-mercaptopropyl) trimethoxysilane (MPTMS) via the thiol-ene click reaction to prepare compressible aerogels (DADMAC-MBAA modified CNF-

silica aerogels). It was demonstrated that the aerogel's maximal MO adsorption capacity was 186.7 mg/g.

In addition, the surface charge properties of aerogels have an effect on dye adsorption. Yi et al. [102] successfully synthesized aramid nanofibers/bacterial cellulose (ANFs/BC) aerogels by a physical gelation process. The aerogel can selectively adsorb cationic dyes in wastewater. Thanks to the hydrophilic and negative charge of the surface. The cationic dye MB was well adsorbed by aerogels, whereas the anionic MO was poorly adsorbed. Figure 3 depicts the adsorption mechanism of ANFs/BC aerogel on dye MB. The dye removal efficiency for MB was 98.8%, much higher compared to the pure BC aerogel (27.9%). Nia et al. [103] synthesized a new silica-cellulose aerogel by chemical cross-linking. The aerogel has a density of 0.107 g/mL, a porosity of approximately 93.0%, and a surface with positively and negatively charged functional groups. The adsorption capacity was 270 mg/g for MB and 300 mg/g for MO. Jiang et al. [104] prepared cellulose nanofibril-based aerogels from TEMPO-oxidized CNF using *tert*-butanol solvent replacement and the freeze-drying method. It is highly effective at removing cationic malachite green dye from water. It has a specific surface area of 193 m²/g and a maximum adsorption of 212.7 mg/g. This happens because the negatively charged carboxylic acid group on the surface attracts the positively charged malachite green (MG) dye. It makes it easier to take out cationic dyes. A new type of adsorption study is also emerging. Yang et al. [105] effectively fabricated a new CO₂-responsive cellulose nanofibril aerogel. When the aerogel received CO₂ stimulation, the aerogel had maximal adsorption capacities of 598.8 mg/g, 621.1 mg/g, and 892.9 mg/g for MB, naphthol green B (NGB), and MO, respectively. It also exhibits excellent recyclability, as it retains its adsorption characteristics even after 20 cycles. Figure 4 depicts the controlled and recyclable dye removal process induced by CO₂.

Table 4 summarizes the performance of nanocellulose-based aerogels in dye removal and compares it with chitosan-based aerogels.

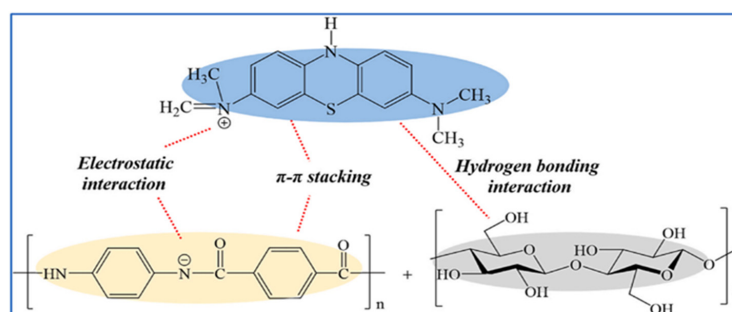


Figure 3. Adsorption mechanism of ANFs/BC aerogel on dye MB [102].

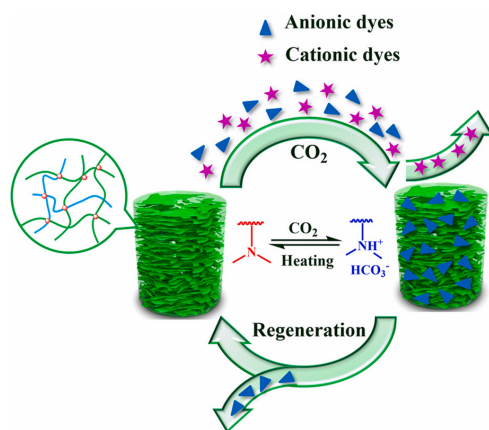


Figure 4. CO₂-responsive cellulose nanofibril aerogel with a controlled and recyclable dye removal process stimulated by CO₂ [105].

Table 4. Performance of nanocellulose-based aerogels in dye removal compared with chitosan-based aerogels. QCSA: quaternized chitosan aerogel; SY: sunset yellow dyes; HPS: chitin/chitosan-based aerogel; ZnBDC/CSC: Zn-MOF/citrate-crosslinked CS.

Aerogel Name	Preparation Method	Dyes	Specific Surface Area (m ² /g)	Porosity (%)	Density (mg/cm ³)	Adsorption Capacity (mg/g)	pH	Number of Cycles	Ref.
Nanocellulose-based aerogels									
Cu-BTC/NFC aerogel	Freeze-drying	CR	18.283	/	/	39	/	/	[66]
CGS	Freeze-drying	MB	/	98.7	19.9	608.4	7	10	[96]
SCP	Freeze-drying	CR MO	/	/	/	2007.48 2253.38	2–5	5	[97]
CNF-GnP	Freeze-drying	MB CR	/	/	/	1178.5 585.3	/	4	[98]
Q-CNF	Freeze-drying	Bule Red Orange	/	99	17.5	230 160 560	/	20	[99]
PCNF	Freeze-drying	MB	368.15	/	27.2	208	5	5	[100]
DADMAC-MBAA modified CNF-Silica aerogels	Freeze-drying	MO	/	/	/	186.7	5–7	3	[101]
ANFs/BC	Freeze-drying	MB	/	/	/	54.45	/	/	[102]
Silica-cellulose aerogel	Freeze-drying	MB MO	350	93	107	270 300	/	/	[103]
Cellulose nanofibril-based aerogel	Freeze-drying	MG	193	/	/	212.7	/	4	[104]
CO ₂ -responsive cellulose nanofibril aerogel	Freeze-drying	MB NGB MO	17.97	/	21.7	598.8 621.1 892.9	/	20	[105]
Chitosan-based aerogels									
QCSA	Freeze-drying	CR MO SY	/	/	60	1259.6 607.5 550.2	7	5	[106]
HPS	Freeze-drying	CR	123.92	98.16	/	2074	6	7	[107]
Fc-CS	Freeze-drying	MB	5	/	/	156.3	5–6	5	[108]
ZnBDC/CSC	Freeze-drying	MO	16.5	/	/	202	5	5	[109]

3.2. Adsorption of Heavy Metal Ions

Heavy metal ions are dangerous to people's health because of their non-biodegradability and tendency to build up in water. Heavy metal ion pollution is often considered one of the most serious contaminants [110,111]. Chemical precipitation, physical adsorption, ion exchange, bioremediation, etc. are all ways to get rid of heavy metal ions [112–114]. Physical adsorption technology is widely used because of its environmental protection and simple preparation process. Therefore, researchers have developed a variety of adsorbent materials. Among them, nanocellulose-based aerogels are the most promising materials owing to their degradability, regenerability, and ease of modification. Lam et al. [115] found that the ability of nanocellulose-based aerogels to hold heavy metals depends mainly on their active sites and porous structure. If the nanocellulose-based aerogels are inherently less hydrophilic and have fewer active sites, they need to be modified. Geng et al. [116] used TEMPO oxidized nanogenic fibrillated cellulose (TO-NFC) and aminopropyltrimethoxysilanes (APTMs) as raw materials. They synthesized 3D macroscopic aminosilylated nanocellulose aerogels (APTMs modified TO-NFC). The research findings indicate that the adsorption capacities of APTMs modified TO-NFC aerogels for Cu^{2+} , Cd^{2+} , and Hg^{2+} were 99.0 mg/g, 124.5 mg/g, and 242.1 mg/g, respectively. Mo et al. [117] prepared three-dimensional layered porous cellulose nanofiber/polyacrylamide composite aerogels by a simple in situ physical/chemical double cross-linking. Figure 5 shows the adsorption mechanism of this composite aerogel and a picture of the cycle of adsorption and regeneration. It could absorb as much as 240 mg/g of Cu^{2+} . Cu^{2+} removal efficiency was maintained at over 80% after 10 cycles of adsorption and regeneration. Wang et al. [118] prepared aerogels with shape memory (MOF@CA) by compounding nanocellulose (CNF) with polyvinyl alcohol (PVA) and a metal organic backbone (MOF). Studies have shown that MOF@CA has a low density (9.8–11.2 mg/cm³), high porosity (99.4–99.5%), and good elasticity in both air and water. MOF@CA had adsorption capabilities of 123 mg/g for Pb^{2+} and 70.53 mg/g for Cu^{2+} , respectively.

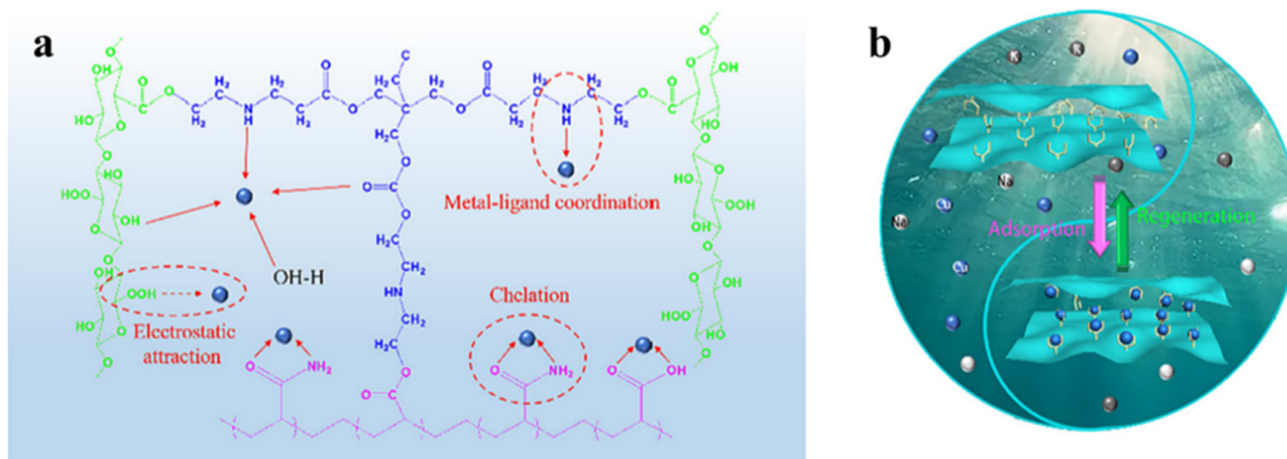


Figure 5. (a) Adsorption mechanism of cellulose nanofiber/polyacrylamide composite aerogel. (b) Graphical illustration of the adsorption-regeneration of Cu^{2+} by cellulose nanofiber/polyacrylamide composite aerogel [117].

Another study, Li et al. [119], made NFC/PEI hybrid aerogels for the adsorption of Cu^{2+} and Pb^{2+} by cross-linking nanofibrillated cellulose (NFC) and polyethyleneimine (PEI) through electrostatic bonding. The greatest levels of Cu^{2+} and Pb^{2+} adsorbed by this aerogel were 175.44 mg/g and 357.44 mg/g, respectively. Guo et al. [120] synthesized a novel polyethyleneimine (PEI)-grafted porous cellulose@PEI aerogel (CPA) by a glutaraldehyde cross-linking process between polyethyleneimine (PEI) amine groups and hydroxyl groups. It was demonstrated that CPA has a maximum adsorption capacity for Cr^{6+} of 229.1 mg/g. Hong et al. [121] prepared PEI@CNF aerogel by grafting polyethyleneimine (PEI) onto the scaffold of cellulose nanofibers (CNFs). Its adsorption capacity for Cu^{2+} was 135.1 mg/g.

In the context of other metal ions, it shows a high selectivity for Cu^{2+} . Several studies have shown that composite aerogels have a stronger adsorption capacity than pure nanocellulose aerogels and maintain structural integrity after multiple applications. Wei et al. [122] integrated ferric tetroxide (Fe_3O_4) nanoparticles and nanocellulose to prepare magnetic hybrid aerogels. The experiments showed that the mixed aerogel adsorption effectiveness for Cr (VI) ions was best. The adsorption process is depicted in Figure 6a. In addition, as shown in Figure 6b, the aerogel was experimentally proved to absorb Pb (II) and Cu (II) from a water solution. Lei et al. [123] synthesized a composite aerogel by combining cellulose with a metal organic backbone (UIO-66- NH_2). It has an equilibrium adsorption capacity of 89.40 mg/g for Pb^{2+} and may be reused without noticeable performance loss for more than 5 cycles. Wang et al. [124] obtained cross-linked CNF aerogels by cross-linking CNFs with polyamide epichlorohydrin resin solution by freeze-drying and vacuum drying. During static uranium adsorption, it displayed rapid adsorption kinetics and a high adsorption capacity (440.60 mg/g). Li et al. [125] developed amine-functionalized cellulose-based aerogel beads (CGP) for effective simultaneous adsorption, reduction, and chelation of Cr (VI). As a result of its high electrostatic attraction to Cr (VI), CGP has a maximum capacity for adsorption of 386.40 mg/g at 25 °C. Shahnaz et al. [126] made composite aerogel (NCNB) by combining customized nanobentonite with nanocellulose/chitosan. Evaluation of its potential to absorb heavy metals from wastewater. It was shown that the aerogel could remove Cr^{6+} , Co^{3+} , and Cu^{2+} with a maximum adsorption efficiency of 98.90%, 97.45%, and 99.01%, respectively.

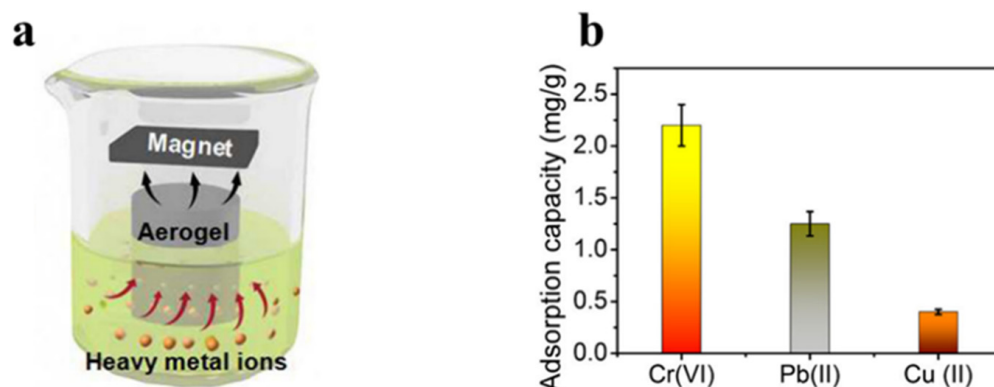


Figure 6. (a) Adsorption behavior of magnetic hybrid aerogels for heavy metal ions under magnetic conditions. (b) Maximum adsorption capabilities of magnetic hybrid aerogels for the absorption of Cr(VI), Pb(II), and Cu(II) ions [122].

Table 5 summarizes the performance of nanocellulose-based aerogels in metal ion removal and compares it with chitosan-based aerogels.

Table 5. Performance of nanocellulose-based aerogels in metal ion removal compared with chitosan-based aerogels. PCA: polyethyleneimine (PEI) functionalized chitosan (CS) aerogel; CSTU: thiourea-chitosan (CSTU) aerogel; WP-CSA: waste paper/chitosan aerogel; E-CS aerogel: enhanced chitosan aerogel; CS-MMT: chitosan-montmorillonite composite aerogel.

Aerogel Name	Preparation Method	Metal Ions	Specific Surface Area (m ² /g)	Porosity (%)	Density (mg/cm ³)	Adsorption Capacity (mg/g)	pH	Number of Cycles	Ref.
Nanocellulose-based aerogels									
APTMs modified TO-NFC	Freeze-drying	Cu (II) Cd (II) Hg (II)	129.32	99.14	/	99 124.5 242.1	3–7	/	[116]
TOCNF-TMPTAP-APAM	Freeze-drying	Cu (II)	/	99.1	14.4	240.00	6	10	[117]
MOF@CA	Freeze-drying	Pb (II) Cu (II)	/	99.4–99.5	9.8–11.2	123.00 70.53	/	5	[118]
NFC/PEI hybrid aerogels	Freeze-drying	Pb (II) Cu (II)	42.5	/	/	357.44 175.44	2–5	3	[119]
CPA	Freeze-drying	Cr (VI)	36.77	/	/	229.10	2	5	[120]
PEI@CNF aerogels	Freeze-drying	Cu (II)	11.48	/	/	135.10	3–6	3	[121]
nanocellulose-Fe ₃ O ₄ hybrid aerogel	Freeze-drying	Cr (II) Pb (II) Cu (II)	/	5	/	2.20 1.25 0.40	/	/	[122]
UiO-66-NH ₂ @CA	Freeze-drying	Pb (II)	/	/	/	89.40	/	5	[123]
CNFs aerogel	Freeze-drying	U (VI)	188	/	/	440.60	5		[124]
CGP	Freeze-drying	Cr (VI)	/	/	/	386.40	2	5	[125]
Chitosan-based aerogels									
PCA	Freeze-drying	Cr (VI)	/	/	/	445.29	3	10	[127]
CSTU	Freeze-drying	Ag (I) Pb (II)	416.64–447.26	/	2.1–10.3	1.11 mmol/g 0.48 mmol/g	6	5	[128]
WP-CSA	Freeze-drying	Cu (II)	/	/	106	156.3	2.3–5.5	/	[129]
E-CS aerogel	Freeze-drying	Cu (II) Pb (II) Cd (II)	/	97.38	38.3	108.14 143.73 84.62	5	3	[130]
CS-MMT	Freeze-drying	Cu (II)	14.133	/	/	86.95	6	7	[131]

3.3. Adsorption of Antibiotics

An antibiotic is an anti-microbial compound. Common antibiotics include macrolides, lincosamides, tetracyclines, phosphate esters, etc. [132]. Antibiotics are mainly sourced from the pharmaceutical industry, hospitals, animal farms, municipal garbage, and wastewater from wastewater treatment plants [133]. Antibiotics are heavily used because of their ability to act specifically on disease-causing bacteria and fungi by killing or inhibiting their growth in human or animal hosts. However, over-application has resulted in large amounts of antibiotics being exposed to the natural environment.

The most common organic micropollutant found in wastewater is antibiotics, posing a severe environmental threat [134]. The application of nanocellulose-based aerogels in antibiotic adsorption has been a research hotspot in recent years. Yao et al. [135] used a one-step ultrasonic technique to create a cellulose nanofiber/graphene oxide hybrid aerogel (CNF/GO). It was utilized for antibiotic adsorption in water. The aerogel achieved a more than 69% removal rate of antibiotics. The adsorption amounts for chloramphenicol, macrolides, quinolones, β -lactams, sulfonamides, and tetracyclines were 418.7 mg/g, 291.8 mg/g, 128.3 mg/g, 230.7 mg/g, 227.3 mg/g, and 454.6 mg/g, respectively. In addition, the aerogel can still be reused after ten cycles with no appreciable loss in adsorption ability. In a separate study, Wang et al. [136] used a one-step ultrasonic approach to create cellulose nanofibrils/graphite oxide hybrid (GO-CNF) aerogels. The aerogel was shown to remove 73.9%, 79.1%, and 81.5%, 79.5% of tetracycline (TC), chlortetracycline (CTC), doxycycline (DXC), and oxytetracycline (OTC), respectively. For TC, CTC, OTC, and DXC, the maximal theoretical adsorption capacities of GO-CNF were 343.8 mg/g, 396.5 mg/g, 386.5 mg/g, and 469.7 mg/g, respectively. In the same study, Wang et al. [137] incorporated cellulose nanofibers (CNFs) into graphene oxide nanosheets by dispersing them. The composite graphene oxide (GO)/cellulose nanogels were then prepared by combining freeze-drying techniques. The adsorption experiments demonstrated that the composite aerogel had a maximum adsorption capacity for TC of 47.3 mg/g. Experiments on adsorption could maintain the removal rate of TC at about 97% after three cycles. Wei et al. [138] will prepare bacterial cellulose (BC) aerogel by freeze-drying technique. Then it was put into a tube furnace for carbonization to finally obtain carbon-bacterial cellulose aerogel (BCCA). At a temperature of 298 K, the maximum adsorption capacities of BCCA for chloramphenicol (CAP), norfloxacin (NOR), and sulfamethoxazole (SMX) were 525 mg/g, 1926 mg/g, and 1264 mg/g, respectively. Liu et al. [139] first obtained modified cellulose (RCA) by chemical-physical double cross-linking with epichlorohydrin (ECH). The RCA was then coated with polyaniline (PANI) via in situ polymerization. Lastly, a metal-organic backbone (ZIF-67) was grown in situ on the PANI-coated modified cellulose to prepare a ZIF-67/PANI/RCA aerogel composite adsorbent. According to the analysis, ZIF-67/PANI/RCA aerogel had an adsorption capability of 409.55 mg/g for TC with good recovery. After six adsorption and desorption cycles, the removal efficiency of TC remained over 94%.

In another study like it, Cui et al. [140] uniformly loaded zeolite imidazole ester skeleton-8 (ZIF-8) onto the surface of cellulose aerogel (CCA) by in situ growth. Finally, it was made into ZIF-8 zeolite cellulose aerogel (ZCCA). It was shown that ZCCA exhibited excellent adsorption performance for enrofloxacin (ENR), besides having a maximal capacity for adsorption of 172.09 mg/g. Ruan et al. [141] first prepared a cellulose nanocrystals (CNCs)/silica (SiO_2) mixture solution. The subsequent step was to add a certain mass fraction of polyvinyl alcohol (PVA) to the mixture of CNCs and SiO_2 . Finally, the freeze-drying approach was utilized to make a PVA-assisted CNC/ SiO_2 aerogel. The research revealed that ciprofloxacin (CIP) was taken up by PVA-assisted CNCs/ SiO_2 composite aerogels mostly through hydrogen bonding, π - π interactions, electrostatic interactions, and hydrophobic interactions. Figure 7 displays the PVA-assisted CNCs/ SiO_2 aerogel adsorption mechanism. The greatest adsorption capacity for CIP in the PVA-assisted CNCs/ SiO_2 aerogel was 163.34 mg/g.

Table 6 demonstrates the performance of nanocellulose-based aerogels for antibiotic removal and compares them with chitosan-based aerogels.

Table 6. Performance of nanocellulose-based aerogels in antibiotic removal compared with chitosan-based aerogels. GO/CNF: GO/nanofibrillated cellulose aerogel; PGO-CS: porous graphene oxide–chitosan aerogel; CMC: carboxymethyl chitosan aerogel; CMC-MT: Na-montmorillonite (Na-Mt) with carboxymethyl chitosan (CMC).

Aerogel Name	Preparation Method	Antibiotics	Specific Surface Area (m ² /g)	Porosity (%)	Adsorption Capacity (mg/g)	pH	Number of Cycles	Ref.
Nanocellulose-based aerogels								
CNF/GO	Freeze-drying	Loramphenicol Macrolides Quinolones β-lactams sulfonamides tetracyclines	97.5	/	418.7 291.8 128.3 230.7 227.3 454.6	2.0	10	[135]
GO-CNF	Freeze-drying	DXC CTC OTC TC	89.9	/	469.7 396.5 386.5 343.8	/	5	[136]
GO/CNF	Freeze-drying	TC	35	/	47.3	/	3	[137]
BCCA	Freeze-drying	CAP NOR SMX	1505	/	525 1926 1264	5	5	[138]
ZIF-67/PANI/RCA aerogel	Freeze-drying	TC	/	/	409.55	7.0	6	[139]
ZCCA	Freeze-drying	ENR	756.45	95	172.09	2.0–6.0	6	[140]
PVA-assisted CNCs/SiO ₂ aerogel	Freeze-drying	CIP	/	/	163.34	4.0	/	[141]
Chitosan-based aerogels								
PGO-CS	Freeze-drying	TC	345	/	1470	9.0–10.0	4	[142]
CMC	Freeze-drying	TC	0.73	/	332.23	3.0–4.0	/	[143]
CMC-Mt	Freeze-drying	CTC	119.526	/	48.71	4.0–7.0	/	[144]

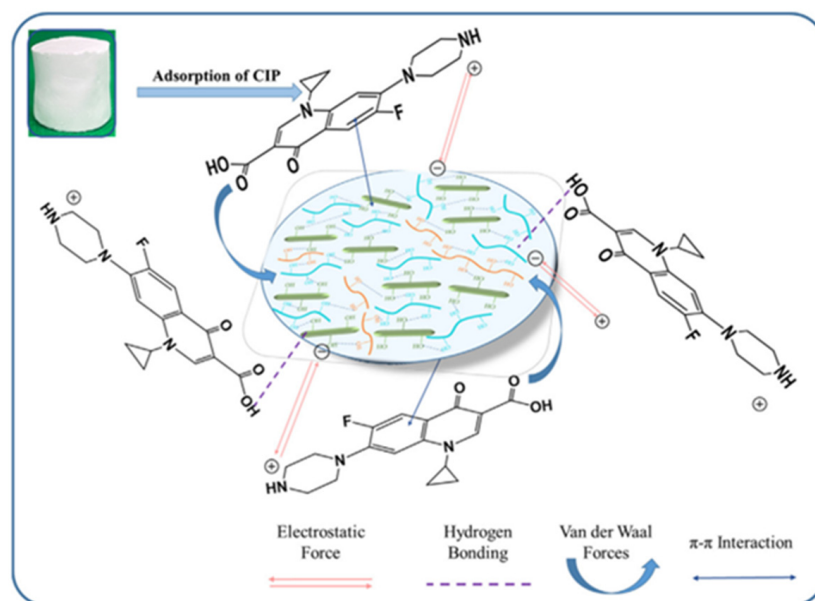


Figure 7. PVA-assisted CNCs/SiO₂ aerogel adsorption mechanism [141].

3.4. Oil-Water Separation and Adsorption of Organic Solvents

Oil pollution has a great impact on the water environment and ecosystems. In addition to oil pollutants, industrial oily wastewater also poses a severe hazard to ecosystems and human health [62]. Organic solvents in wastewater generally originate from the textile, printing leather, and chemical industries, as well as from the cleaning and polishing of furniture components. Such as benzonitrile, chloroform, glycol ether, methylene chloride, acetone, toluene, ethylbenzene, and xylene [145]. Organic solvents in water, like oil, can damage the marine environment and have a serious impact on the survival of aquatic and terrestrial plants and animals [146]. Oil pollution and organic solvents pose substantial harm to ecosystems, human life, economies, etc. Common methods used to clean up petroleum contamination and organic solvents include in-situ combustion, mechanical methods, chemical treatment, bioremediation, and adsorption [147]. The adsorption method is considered an economic and effective method to deal with oil contamination and organic solvents [145]. Because it costs less to make, uses less energy, and does not cause secondary contamination. The advantages of naturally renewable, biodegradable, high porosity, and easy surface modification of nanocellulose-based aerogels. It can be used as a natural adsorbent.

However, because nanocellulose-based aerogels have natural hydroxyl groups on the surface, these hydrophilic groups reduce the adsorption of oily substances and organic solvents. To solve this problem, we usually modify the surface of nanocellulose-based aerogels to increase their hydrophobicity. The hydrophobic function of high-nanofiber-based aerogels is commonly achieved by silylation. Akhlamadi et al. [148] first cross-linked cellulose nanocrystals (CNC) with polyvinyl alcohol (PVA). Then, among them, tetraethyl orthosilicate (TEOS) was added dropwise to prepare silylated PVA/CNC aerogels after freeze-drying. The adsorption experiments demonstrated that the silanized PVA/CNC aerogels showed 69 to 168 g/g adsorption capacity for six oils and eight organic solvents (as shown in Figure 8) and were reusable. After 20 adsorption-extrusion cycles, the aerogel retains more than 92% of its adsorption capacity. The aerogel may be utilized as a reusable adsorbent. Rosli et al. [149] modified cellulose nanocrystals (CNC) from kenaf fibers using methyltrimethoxysilane (MTMS) and combined with γ -irradiated cross-linked gelatin. The γ -irradiated modified cellulose nanocrystals/gelatin aerogels (γ -irradiated CNC-MTMS/gelatin aerogels) were then prepared using the sol-gel method. Its water contact angle (WCA) is 118°. It is shown that the aerogel can absorb crude oil up to 430% of its own weight with good reproducibility. By the eighth cycle, the crude oil uptake

had been reduced by only 4%. Zhang et al. [150] used vinyltrimethoxysilane (VTMO) to modify microfibrillated cellulose (MFC). Chopped kapok fiber powder was added to it, followed by the freeze-drying method. High-porosity (99.58%) and hydrophobicity (140.1°) kapok/microfibrillated cellulose aerogels (KCAs) were developed. KCAs have an ultra-high absorption capacity of 104–190.1 g/g, a high retention capacity (of 97%), and a fast oil absorption rate (of 0.74 g/s). Even after 10 uses, it still has a high capacity to soak up oil. Wang et al. [151] used methyltrichlorosilane (MTS) to modify the cellulose nanocrystals. Hydrophobic and lipophilic cellulose nanocrystal (CNC) aerogels (MTS-CNC) were then prepared by gas-phase reactions. MTS-CNC has a high contact angle of 148.5° and a maximum adsorption capacity of 60 g/g for paraffin oil. Qiao et al. [152] placed cellulose nanofibers (CNF) into a polydimethylsiloxane (PDMS) solution for soaking and heat treatment. Cellulose nanofiber (CNF-PDMS) aerogel sheets and blocks with efficient oil/water separation were obtained using directional freeze-drying. CNF-PDMS aerogel sheets can achieve continuous filtration separation of oil and water with a separation efficiency of 99.9%. CNF-PDMS aerogel blocks can separate oil and water mixtures by adsorption and extrusion. It can also be applied to vacuum suction for real-time continuous oil-water separation with a separation efficiency of 99.9%. Figure 9 is a schematic of oil-water separation and CNF-PDMS aerogel sheet and block construction. Mi et al. [153] modified cellulose nanofilaments (CNF) by perfluorododecyltriethoxysilane (PDTs) surface modification combined with the freeze-drying method. They combined organic cellulose nanofilaments (CNF), inorganic silica fibers, and magnetic Fe_3O_4 nanoparticles to create a novel ultra-lightweight and superhydrophobic nanocomposite aerogel (M-CNF/silica/ Fe_3O_4). The aerogel has a high absorption capacity (3420%–5837%) above its own weight, a separation efficiency of 100%, and a WCA of 150° . Liu et al. [154] mixed cellulose nanofibers (CNF) with sodium alginate (SA) and surface-modified by ionic cross-linking and methyltrimethoxysilane (MTMS). Cellulose nanofibers/alginate aerogels (CNF/SA) with a WCA of 144.5° and high porosity (97.85%) were prepared by combining bi-directional freeze-drying. This aerogel possesses a high oil absorption capacity (nearly 88.91 g/g) and is reusable for continuous oil-water separation. It can effectively solve the problem of a marine oil spill. Zhang et al. [155] added vinyltrimethoxysilane (VTMO) and cotton fibers to a cellulose nanofiber (CNF) suspension. After freeze-drying to obtain the wood cotton/cellulose nanofiber aerogel (KNA). Studies have shown that KNA aerogels exhibit high oil absorption (141.9 g/g) as well as outstanding selective adsorption performance. This makes it an ideal sorbent for cleaning oil spills.

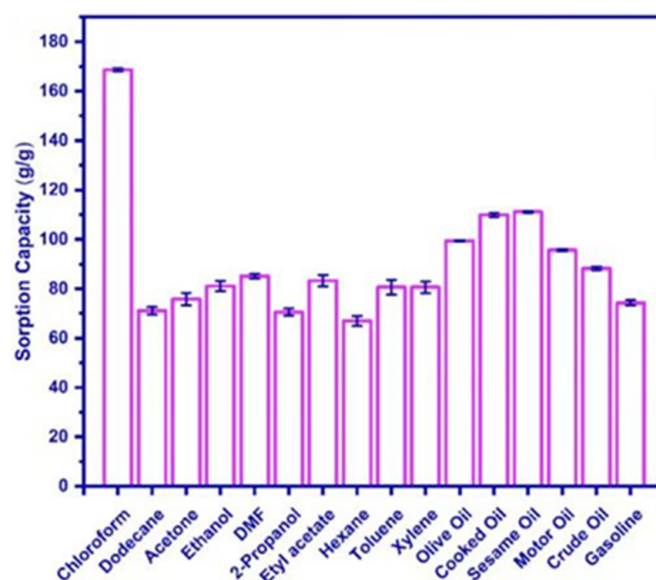


Figure 8. Adsorption capacity of silanized PVA/CNC aerogel [148].

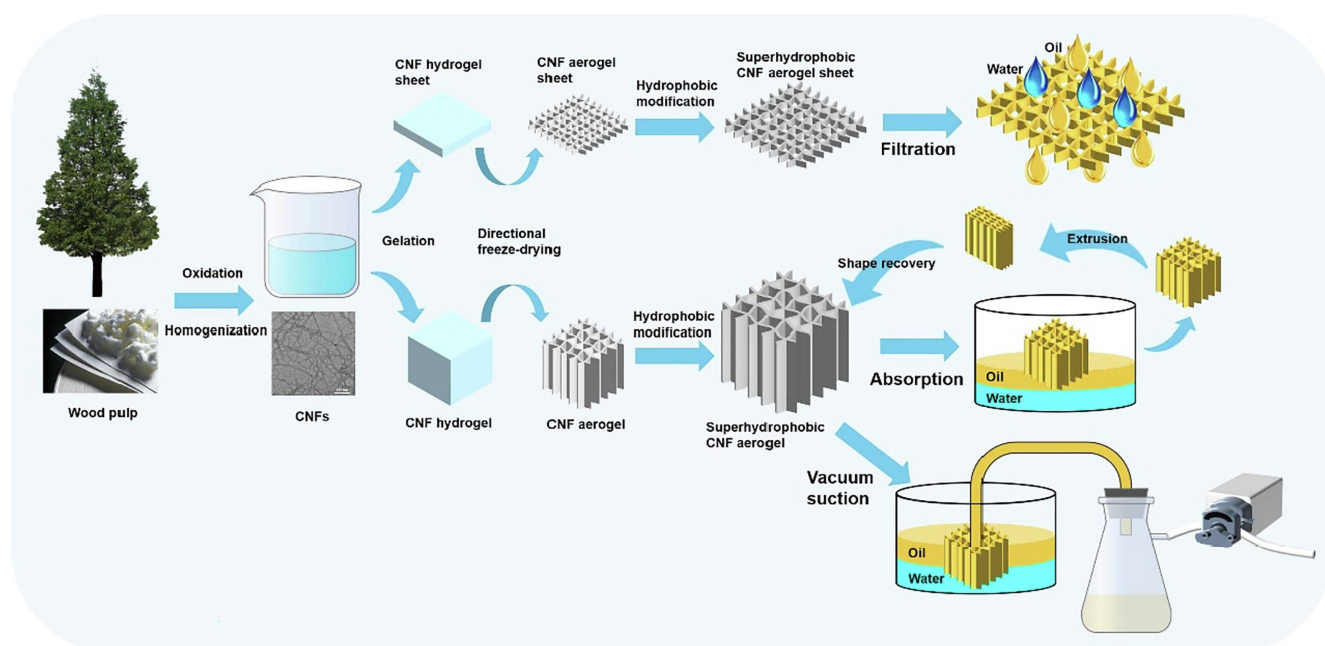


Figure 9. Preparation and oil-water separation diagrams of CNF-PDMS aerogel sheets and blocks [152].

There are some other modification methods in the study to make nanocellulose-based aerogels for oil-water separation and the adsorption of organic solvents. To increase the hydrophobicity and the adsorption capacity of nanocellulose (NC) aerogels, Gu et al. [156] prepared NC/NCS/rGO nanocomposite aerogels by introducing reduced graphene oxide (rGO) and nanochitosan (NCS) into NC aerogels by a hydrothermal method combined with freeze-drying. The experiments demonstrated that the adsorption capabilities of the aerogel for acetone, sesame oil, ethyl acetate, mineral oil, thiophene, pump oil, used pump oil, kerosene, and ethanol were 153.22 ± 2.92 g/g, 159.64 ± 1.83 g/g, 149.60 ± 6.26 g/g, 171.85 ± 3.02 g/g, 139.93 ± 3.69 g/g, 132.47 ± 3.45 g/g, 176.82 ± 4.66 g/g, 128.70 ± 0.69 g/g, and 120.34 ± 5.57 g/g. NC/NCS/rGO nanocomposite aerogels may effectively remove oil and organic solvents from wastewater. Wang et al. [157] created TOCN aerogels from TEMPO-oxidized cellulose nanofibers (TOCN) by freeze-drying. It was transferred to a tube furnace for carbonization to finally obtain TOCN carbon aerogel. It has been shown that TOCN carbon aerogels have demonstrated superior oil/water selectivity and high absorption. The maximum absorption capacity ranges between 110 g/g and 260 g/g based on the organic solvent density.

In a similar study, Ma et al. [158] added cotton slurry to lithium bromide (LiBr) and stirred it to form a gel after cooling. Then aerogel was prepared by freeze-drying. Finally, the aerogel was put into a tube furnace for carbonization to prepare cellulose carbon aerogel (CCA). The produced aerogel exhibited excellent hydrophobicity (WCA over 135°). It can adsorb up to 55 times its own weight in pump oil. In addition, CCA is reusable, as its ability to absorb oil and organic solvents can be restored to more than 90% of its original capacity after five cycles. Zhou et al. [159] prepared NC/Al₂O₃ aerogels by mixing nanocellulose (NC) and nanoalumina (Al₂O₃) in deionized water and freeze-drying them. As illustrated in Figure 10, the NC/Al₂O₃ aerogel had high adsorption capability for anhydrous ethanol, ethyl acetate, thiophene, cyclohexane, sesame oil, acetone, and dichloromethane in experimental conditions. The adsorption capabilities were 89.91 ± 4.83 g/g, 93.93 ± 3.81 g/g, 108.07 ± 0.37 g/g, 71.13 ± 2.48 g/g, 64.83 ± 2.25 g/g, 85.19 ± 3.87 g/g, and 117.65 ± 5.68 g/g, respectively.

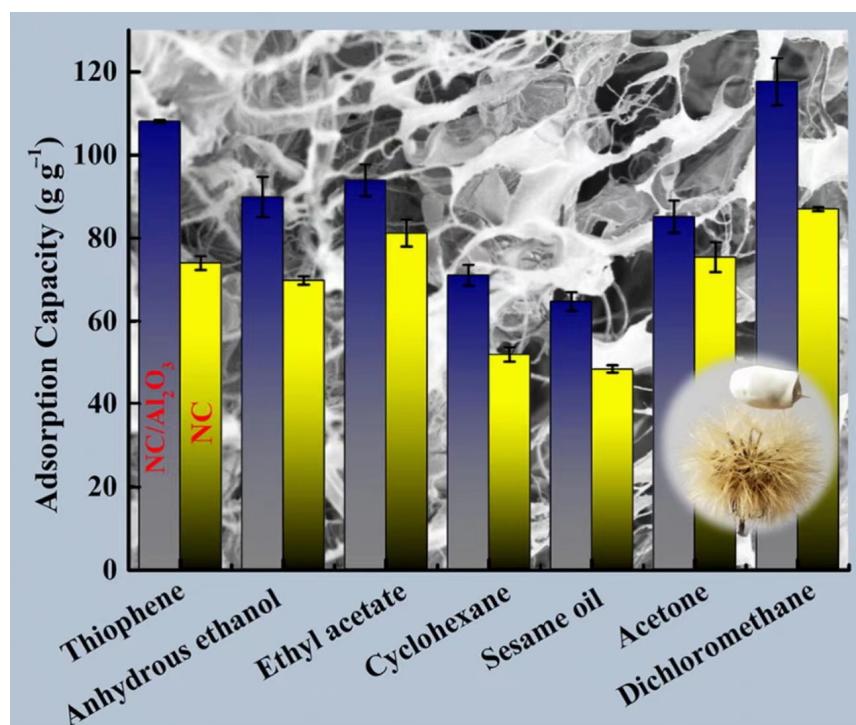


Figure 10. Adsorption capacity of NC/Al₂O₃ aerogel [159].

Chhajed et al. [160] prepared hydrophobic aerogels (NLA) by mixing nanocellulose and natural rubber latex (NRL) using the direct mixing method. The WCA of the obtained samples was about 120.5°, with a porous structure that self-assembled. The aerogels had an adsorption capacity of 30–67 g/g in oil/organic solvents and were reused with 85% efficiency for at least 10 cycles. Fan et al. [161] prepared antimicrobial poly (APDMH)-g-ONC (PAC) by grafting 3-(3'-propyl acrylate)-5,5-dimethylglycolide (APDMH) onto oxidized NFC (ONC). PAC and polyethyleneimine (PEI) were chemically cross-linked using 3-glycidoxypopyl trimer (GPTMS). They made PAC-g-PEI aerogels with different kinds of network structures. The schematic diagram of oil-water separation of PAC-g-PEI aerogel is shown in Figure 11. Studies have shown that PAC-g-PEI aerogel achieves greater than 99% oil/water separation efficiency, in excess of 9500 L·m⁻²·h⁻¹ of flux. It has a good fatigue resistance of more than fifty compression cycles and a good elasticity of 96.76% height recovery after five compression release cycles at fifty percent strain. Zhang et al. [162] prepared a nanocellulose hybrid aerogel (P-CNS) by UV-induced thiol click reactions. P-CNS aerogel has a high surface area (362.7 m²/g) and has adsorption properties on various oils/organic solvents (dichloromethane, soybean oil, pump oil, chloroform, diesel, motor oil, ethanol, acetone, toluene, hexane, gasoline, and octane). The adsorption capacity is 100 to 225 g/g. Zhang et al. [163] successfully synthesized quaternized N-haloamine siloxane monomers. Moreover, blended it with nanocrystalline cellulose (NCC) and chitosan (CS) to prepare efficient oil/water separation and antibacterial aerogels. This aerogel has a high porosity (≥97.66%) and a high separation efficiency (over 99.9%). It has some inhibitory effects on bacteria in oily wastewater.

Table 7 shows the performance of nanocellulose-based aerogels in separating oil/organic solvents and compares them with chitosan-based aerogels.

Table 7. Performance of nanocellulose-based aerogels compared with chitosan-based aerogels for oil/organic solvent separation. PNI-Si@CCNT/CA: vinyltrimethoxysilane and thermally responsive poly(N-isopropylacrylamide) (PNIPAAm) were grafted onto the surface of a carboxylated carbon nanotube/chitosan aerogel backbone to obtain aerogels; CA/CS/CMC: citric acid/chitosan/carboxymethyl cellulose aerogel; DMF: dimethylformamide; THF: tetrahydrofuran; DMSO: dimethyl sulfoxide; DCM: dichloromethane.

Aerogel Name	Preparation Method	Oil/Organic Solvents	Specific Surface Area (m ² /g)	Porosity (%)	Density (mg/cm ³)	Adsorption Capacity (g/g)	Water Contact Angle (°)	Number of Cycles	Ref.
Nanocellulose-based aerogels									
silylated PVA/CNC aerogels	Freeze-drying	Chloroform Dodecane Acetone Ethanol DMF 2-Propanol Etyl acetate Hexane Toluene Xylene Olive oil Cooked oil Sesame oil Motor oil Crude oil Gasoline	76	98.42	17	69–168	154.93	20	[148]
γ -irradiated CNC-MTMS/gelatin aerogels	Freeze-drying	Chloroform Crude oil	/	/	85	/ (It can absorb 430% of its own weight)	118	8	[149]
KCAs	Freeze-drying	Vegetable Oil Motor oil Gasoline Vacuum pump oil Trichloromethane Ethanol DMF	/	99.58	5.1	104–190.2	140.1	10	[150]
MTS-CNC	Freeze-drying	Liquid paraffin oil	282	/	/	60	148.5	5	[151]

Table 7. Cont.

Aerogel Name	Preparation Method	Oil/Organic Solvents	Specific Surface Area (m ² /g)	Porosity (%)	Density (mg/cm ³)	Adsorption Capacity (g/g)	Water Contact Angle (°)	Number of Cycles	Ref.
CNF-PDMS	Freeze-drying	Dim ethyl benzene Ethyl acetate Ethanol n-Hexane n-Decane n-Dodecane n-Hexadecane Methylcyclohexane Dichloroethane Toluene Dimethylformamide Petroleum ether THF Petroleum	/	98.4	22.7	24–48	163.5	20	[152]
M-CNF/silica/Fe ₃ O ₄)	Freeze-drying	DMF DMSO Octane Gasoline Dioxane Toluene Hexane Chloroform	82.6	/	22.3	34–58	150	10	[153]
CNF/SA	Freeze-drying	Flax seed oil Pump oil Used pump oil Olive oil Silicane oil Toluene Acetone Ethanol Hexane Ethylene glycol DMF DMSO	149.64	97.85	24.2	41.16–88.91	144.5	20	[154]
KNA	Freeze-drying	vegetable oil	/	99.5–99.6	4.9–6.0	141.9	147.6	/	[155]

Table 7. Cont.

Aerogel Name	Preparation Method	Oil/Organic Solvents	Specific Surface Area (m ² /g)	Porosity (%)	Density (mg/cm ³)	Adsorption Capacity (g/g)	Water Contact Angle (°)	Number of Cycles	Ref.
NC/NCS/rGO nanocomposite aerogel	Freeze-drying	Acetone	/	99.18	/	153.22	115.26	/	[156]
		Sesame oil				159.64			
		Ethyl acetate				149.60			
		Mineral oil				171.85			
		Thiophene Pump oil				139.93			
		Used pump oil				132.47			
		Kerosene				176.82			
		Ethanol				128.70			
TOCN carbon aerogel	Freeze-drying and high-temperature carbonization	Gasoline	249.91	99.5	8.8	110–260	139.6	5	[157]
		Diesel oil							
		Pump oil							
		Motor oil							
		Sesame oil							
		Chloroform							
		Acetaldehyde							
		Ethanol							
		Toluene							
		Octadecylene							
		Cyclohexane							
		Heptane							
		n-Hexane							
		Acetone							
		Methanol							
		Lactic acid							
Styrene									
THF									
DMF									
CCA	Freeze-drying and high-temperature carbonization	Soybean oil	79.2	98.9–99.2	16–23	22–55	>135	5	[158]
		Pump oil							
		Acetone							
		Ethylene glycol							
		Methanol							
		DMF							
Hexane									
Ethanol									

Table 7. Cont.

Aerogel Name	Preparation Method	Oil/Organic Solvents	Specific Surface Area (m ² /g)	Porosity (%)	Density (mg/cm ³)	Adsorption Capacity (g/g)	Water Contact Angle (°)	Number of Cycles	Ref.
NC/Al ₂ O ₃ aerogel	Freeze-drying	Anhydrous ethanol Ethyl acetate Thiophene Cyclohexane Sesame oil Acetone Dichlormethae	124	99.09	5.1	89.91 93.93 108.07 71.13 64.83 85.19 117.65	/	/	[159]
NLA	Freeze-drying	Crude oil Rexid oil Silicon oil Vacuum pump oil Red oil Hexane Xylene DMF THF DCM Chloroform	/	98	22	30–67	120.5	10	[160]
PAC-g-PEI	Freeze-drying	n-hexane toluene edible oil silicone oil	/	94	67	/ (Separation efficiency over 99%)	/ (Oil contact angle is 130.3°–135°)	50	[161]
P-CNS	Freeze-drying	Dichloromethae Soybean oil Pump oil Chloroform Diesel Motor oil Ethanol Acetone Toluene Hexane Gasoline Octane	362.7	98.9–99.4	8.4–12.9	100–225	133.6–168.4	50	[162]
NCC/CS aerogel	Freeze-drying	Methylbenzene Petroleum ether n-Hexane Edible oil Silicone oil Dodecane	/	97.66	40.82	/ (Separation efficiency over 99%)	/ (Oil contact angle is 109°–141.1°)	50	[163]

Table 7. Cont.

Aerogel Name	Preparation Method	Oil/Organic Solvents	Specific Surface Area (m ² /g)	Porosity (%)	Density (mg/cm ³)	Adsorption Capacity (g/g)	Water Contact Angle (°)	Number of Cycles	Ref.
Chitosan-based aerogels									
PNI-Si@CCNT/CA	Freeze-drying	N-hexane	2.81	/	0.0051	23.8	/ (Oil contact angle is 134°)	9	[164]
		Toluene				35.3			
		Trichloromethane				53.0			
		Petroleum ether				42.1			
		Peanut oil				41.0			
		Soybean oil				35.2			
		Sunflower oil				32.5			
Olive oil	40.8								
CsA	Freeze-drying	Crude oil	28.3	97.98	28.3	41.07	/	3.0–4.0	[165]
		Diesel				31.07			
(CA/CS/CMC)	Freeze-drying	Chloroform Toluene Acetone Methanol Ethanol	/	96	8.3–63.6	27–44	/	4.0–7.0	[166]



Figure 11. Schematic diagram of oil-water separation of PAC-g-PEI gas coagulant [161]. Reprinted (adapted) with permission from (Fan, B.; Qi, B.; Wang, P.; Liu, Y.; Yu, Y.; Wang, Q.; Ren, X. Mechanically Tough and Regenerable Antibacterial Nanofibrillated Cellulose-Based Aerogels for Oil/Water Separation. *Langmuir* 2022, 38, 10716–10727.) Copyright American Chemical Society.

4. Conclusions and Perspectives

Nanocellulose-based aerogel as an emerging porous material. It not only has the three-dimensional structure, high specific surface area, light weight, and high porosity of traditional inorganic aerogel materials. It also has the unique advantages of high biocompatibility, degradability, easy surface modification, good mechanical strength, etc. Nanocellulose-based aerogels with a highly porous three-dimensional network structure exhibit excellent adsorption properties, mechanical strength, and reusability for hazardous substances (dyes, heavy metal ions, petroleum, organic solvents, and antibiotics) in wastewater. As well as the advantages of nanocellulose-based aerogel, such as environmental protection, low cost, a wide source of raw materials, and mechanical durability. Making it significantly better than other adsorbent materials. In addition, 2D nanomaterials such as graphene oxide (GO) and metal organic backbone (MOF) were found to be combined with nanocellulose-based aerogels. Because of the increased porosity and total area, the adsorption characteristics of nanocellulose-based aerogels can be greatly enhanced. Although nanocellulose-based aerogels show excellent performance under harsh conditions and exhibit strong affinity for various hazardous substances in wastewater. However, the application of nanocellulose-based aerogels in wastewater is not without obstacles, and there are still some obstacles to overcome as follows. Here are some key challenges and suggestions for the future:

1. The production of nanocellulose-based aerogels is a complex procedure. Each preparation condition needs to be controlled in order to obtain high-quality products. Moreover, the preparation cost is high, the solvent replacement is time-consuming, and the drying process is complicated. Simpler and more economical methods should be developed to reduce time, cost, energy consumption, and the need for toxic chemicals.

2. Most of the current research on nanocellulose-based aerogels has been carried out in the laboratory. Therefore, the potential of nanocellulose-based aerogels for practical wastewater treatment in industry needs to be evaluated.

3. The regeneration and reuse of nanocellulose-based aerogels is an important issue. Although aerogels can be regenerated and reused by heat treatment, chemical treatment, etc. However, its regeneration effect and utilization times are affected by many factors, such as pollutant type, adsorption amount, regeneration method, etc. Therefore, more economical and efficient methods for regeneration and reuse of aerogels need to be sought to improve the efficiency of aerogel use.

4. The stability and persistence of nanocellulose-based aerogels also need to be further improved. To ensure its stability and adsorption effect during long-term use.

5. The large variety of pollutants in wastewater and the large variation in concentration make it difficult to ensure the adsorption effect of aerogel. In order to address this issue, targeted studies are needed for different types of pollutants.

6. In addition to the variety of pollutants in wastewater, there are also various bacteria present. Therefore, there is a need to further improve the functionality (e.g., antimicrobial properties) of the nanocellulose-based aerogels. So that it has both adsorption capacity to adsorb pollutants and antimicrobial properties to resist bacteria in the wastewater environment.

7. The adsorption mechanism of nanocellulose-based aerogels should be analyzed in more depth. Adequate understanding of the interaction between contaminant molecules and aerogels is needed. This is more conducive to promoting the use of nanocellulose-based aerogels for the removal of new contaminants that may emerge in the water environment in the future.

Author Contributions: Conceptualization, J.Z., X.Y., X.W. and L.L.; methodology, J.Z., X.Y., X.W. and L.L.; writing—original draft preparation, J.Z.; writing—review and editing, K.X., H.G., G.D. and L.Z. All authors have read and agreed to the published version of the manuscript.

Funding: This work is supported by the Natural Science Foundation of China (22161043 and 21801096), the Yunnan Fundamental Research Project (202201AU070071 and 202201AT070453), the Natural Science Foundation of Zhejiang Province (LY21B020009), the “High-level Talent Introduction Program” Project of Yunnan Province (YNQR-QNRC-2019-065), the Innovation and Entrepreneurship Training Program for College Students in Yunnan Province (20201364003), the Startup Funding of Southwest Forestry University (112126), and the 111 Project (D21027).

Institutional Review Board Statement: Not applicable.

Informed Consent Statement: Not applicable.

Data Availability Statement: Not applicable.

Conflicts of Interest: The authors declare no competing financial interests or personal relationships that could have appeared to influence the work reported in this paper.

Sample Availability: Samples of the compounds are not available from the authors.

References

1. Garrick, D.E.; Hall, J.W.; Dobson, A.; Damania, R.; Grafton, R.Q.; Hope, R.; Hepburn, C.; Bark, R.; Boltz, F.; De Stefano, L. Valuing water for sustainable development. *Science* **2017**, *358*, 1003–1005. [[CrossRef](#)] [[PubMed](#)]
2. Abdellatif, F.H.H.; Abdellatif, M.M. Bio-based i-carrageenan aerogels as efficient adsorbents for heavy metal ions and acid dye from aqueous solution. *Cellulose* **2020**, *27*, 441–453. [[CrossRef](#)]
3. Janani, R.; Gurunathan, B.; Sivakumar, K.; Varjani, S.; Ngo, H.H.; Gnansounou, E. Advancements in heavy metals removal from effluents employing nano-adsorbents: Way towards cleaner production. *Environ. Res.* **2022**, *203*, 111815.
4. Lima, E.C. Removal of emerging contaminants from the environment by adsorption. *Ecotoxicol. Environ. Saf.* **2018**, *150*, 1–17.
5. Bhatia, D.; Sharma, N.R.; Singh, J.; Kanwar, R.S. Biological methods for textile dye removal from wastewater: A review. *Crit. Rev. Environ. Sci. Technol.* **2017**, *47*, 1836–1876. [[CrossRef](#)]
6. Roy, M.; Saha, R. Dyes and their removal technologies from wastewater: A critical review. *Intell. Environ. Data Monit. Pollut. Manag.* **2021**, *2021*, 127–160.
7. Hokkanen, S.; Bhatnagar, A.; Sillanpää, M. A review on modification methods to cellulose-based adsorbents to improve adsorption capacity. *Water Res.* **2016**, *91*, 156–173. [[CrossRef](#)]
8. Mahfoudhi, N.; Boufi, S. Nanocellulose as a novel nanostructured adsorbent for environmental remediation: A review. *Cellulose* **2017**, *24*, 1171–1197. [[CrossRef](#)]
9. Hasanpour, M.; Hatami, M. Application of three dimensional porous aerogels as adsorbent for removal of heavy metal ions from water/wastewater: A review study. *Adv. Colloid Interface Sci.* **2020**, *284*, 102247. [[CrossRef](#)]
10. Fan, Y.; Ma, W.; Han, D.; Gan, S.; Dong, X.; Niu, L. Convenient recycling of 3D AgX/graphene aerogels (X= Br, Cl) for efficient photocatalytic degradation of water pollutants. *Adv. Mater.* **2015**, *27*, 3767–3773. [[CrossRef](#)]
11. García-González, C.A.; Alnaief, M.; Smirnova, I. Polysaccharide-based aerogels—Promising biodegradable carriers for drug delivery systems. *Carbohydr. Polym.* **2011**, *86*, 1425–1438. [[CrossRef](#)]
12. Kistler, S.S. Coherent expanded aerogels and jellies. *Nature* **1931**, *127*, 741. [[CrossRef](#)]

13. Zhang, Y.-G.; Zhu, Y.-J.; Xiong, Z.-C.; Wu, J.; Chen, F. Bioinspired ultralight inorganic aerogel for highly efficient air filtration and oil–water separation. *ACS Appl. Mater. Interfaces* **2018**, *10*, 13019–13027. [[CrossRef](#)] [[PubMed](#)]
14. Liu, Z.; Ran, Y.; Xi, J.; Wang, J. Polymeric hybrid aerogels and their biomedical applications. *Soft Matter* **2020**, *16*, 9160–9175. [[CrossRef](#)] [[PubMed](#)]
15. Cao, L.; Si, Y.; Wu, Y.; Wang, X.; Yu, J.; Ding, B. Ultralight, superelastic and bendable lashing-structured nanofibrous aerogels for effective sound absorption. *Nanoscale* **2019**, *11*, 2289–2298. [[CrossRef](#)]
16. Zhang, X.; Liu, M.; Wang, H.; Yan, N.; Cai, Z.; Yu, Y. Ultralight, hydrophobic, anisotropic bamboo-derived cellulose nanofibrils aerogels with excellent shape recovery via freeze-casting. *Carbohydr. Polym.* **2019**, *208*, 232–240. [[CrossRef](#)]
17. Qi, J.; Xie, Y.; Liang, H.; Wang, Y.; Ge, T.; Song, Y.; Wang, M.; Li, Q.; Yu, H.; Fan, Z. Lightweight, flexible, thermally-stable, and thermally-insulating aerogels derived from cotton nanofibrillated cellulose. *ACS Sustain. Chem. Eng.* **2019**, *7*, 9202–9210. [[CrossRef](#)]
18. Tan, K.; Heo, S.; Foo, M.; Chew, I.M.; Yoo, C. An insight into nanocellulose as soft condensed matter: Challenge and future prospective toward environmental sustainability. *Sci. Total Environ.* **2019**, *650*, 1309–1326. [[CrossRef](#)]
19. Kargazadeh, H.; Mariano, M.; Gopakumar, D.; Ahmad, I.; Thomas, S.; Dufresne, A.; Huang, J.; Lin, N. Advances in cellulose nanomaterials. *Cellulose* **2018**, *25*, 2151–2189. [[CrossRef](#)]
20. Yuan, X.; Zhao, J.; Wu, X.; Yao, W.; Guo, H.; Ji, D.; Yu, Q.; Luo, L.; Li, X.; Zhang, L. Extraction of Corn Bract Cellulose by the Ammonia-Coordinated Bio-Enzymatic Method. *Polymers* **2022**, *15*, 206. [[CrossRef](#)]
21. Abitbol, T.; Rivkin, A.; Cao, Y.; Nevo, Y.; Abraham, E.; Ben-Shalom, T.; Lapidot, S.; Shoseyov, O. Nanocellulose, a tiny fiber with huge applications. *Curr. Opin. Biotechnol.* **2016**, *39*, 76–88. [[CrossRef](#)] [[PubMed](#)]
22. Bian, H.; Luo, J.; Wang, R.; Zhou, X.; Ni, S.; Shi, R.; Fang, G.; Dai, H. Recyclable and reusable maleic acid for efficient production of cellulose nanofibrils with stable performance. *ACS Sustain. Chem. Eng.* **2019**, *7*, 20022–20031. [[CrossRef](#)]
23. Badshah, M.; Ullah, H.; Khan, S.A.; Park, J.K.; Khan, T. Preparation, characterization and in-vitro evaluation of bacterial cellulose matrices for oral drug delivery. *Cellulose* **2017**, *24*, 5041–5052. [[CrossRef](#)]
24. Picheth, G.F.; Pirich, C.L.; Sierakowski, M.R.; Woehl, M.A.; Sakakibara, C.N.; de Souza, C.F.; Martin, A.A.; da Silva, R.; de Freitas, R.A. Bacterial cellulose in biomedical applications: A review. *Int. J. Biol. Macromol.* **2017**, *104*, 97–106. [[CrossRef](#)]
25. Bian, H.; Dong, M.; Chen, L.; Zhou, X.; Wang, R.; Jiao, L.; Ji, X.; Dai, H. On-demand regulation of lignocellulosic nanofibrils based on rapid fractionation using acid hydrotrope: Kinetic study and characterization. *ACS Sustain. Chem. Eng.* **2020**, *8*, 9569–9577. [[CrossRef](#)]
26. Bian, H.; Chen, L.; Dong, M.; Wang, L.; Wang, R.; Zhou, X.; Wu, C.; Wang, X.; Ji, X.; Dai, H. Natural lignocellulosic nanofibril film with excellent ultraviolet blocking performance and robust environment resistance. *Int. J. Biol. Macromol.* **2021**, *166*, 1578–1585. [[CrossRef](#)]
27. Kobayashi, Y.; Saito, T.; Isogai, A. Aerogels with 3D ordered nanofiber skeletons of liquid-crystalline nanocellulose derivatives as tough and transparent insulators. *Angew. Chem. Int. Ed.* **2014**, *53*, 10394–10397. [[CrossRef](#)]
28. Habibi, Y.; Lucia, L.A.; Rojas, O.J. Cellulose nanocrystals: Chemistry, self-assembly, and applications. *Chem. Rev.* **2010**, *110*, 3479–3500. [[CrossRef](#)]
29. Klemm, D.; Kramer, F.; Moritz, S.; Lindström, T.; Ankerfors, M.; Gray, D.; Dorris, A. Nanocelluloses: A new family of nature-based materials. *Angew. Chem. Int. Ed.* **2011**, *50*, 5438–5466. [[CrossRef](#)]
30. Gorgieva, S.; Trček, J. Bacterial cellulose: Production, modification and perspectives in biomedical applications. *Nanomaterials* **2019**, *9*, 1352. [[CrossRef](#)]
31. Pakutsah, K.; Aht-Ong, D. Facile isolation of cellulose nanofibers from water hyacinth using water-based mechanical defibrillation: Insights into morphological, physical, and rheological properties. *Int. J. Biol. Macromol.* **2020**, *145*, 64–76. [[CrossRef](#)] [[PubMed](#)]
32. Xue, J.; Zhu, E.; Zhu, H.; Liu, D.; Cai, H.; Xiong, C.; Yang, Q.; Shi, Z. Dye adsorption performance of nanocellulose beads with different carboxyl group content. *Cellulose* **2022**, *30*, 1623–1636. [[CrossRef](#)]
33. Chen, Q.; Liu, Y.; Chen, G. A comparative study on the starch-based biocomposite films reinforced by nanocellulose prepared from different non-wood fibers. *Cellulose* **2019**, *26*, 2425–2435. [[CrossRef](#)]
34. Wen, Y.; Yuan, Z.; Liu, X.; Qu, J.; Yang, S.; Wang, A.; Wang, C.; Wei, B.; Xu, J.; Ni, Y. Preparation and characterization of lignin-containing cellulose nanofibril from poplar high-yield pulp via TEMPO-mediated oxidation and homogenization. *ACS Sustain. Chem. Eng.* **2019**, *7*, 6131–6139. [[CrossRef](#)]
35. Sun, X.; Wu, Q.; Ren, S.; Lei, T. Comparison of highly transparent all-cellulose nanopaper prepared using sulfuric acid and TEMPO-mediated oxidation methods. *Cellulose* **2015**, *22*, 1123–1133. [[CrossRef](#)]
36. Coseri, S.; Biliuta, G.; Simionescu, B.C.; Stana-Kleinschek, K.; Ribitsch, V.; Harabagiu, V. Oxidized cellulose—Survey of the most recent achievements. *Carbohydr. Polym.* **2013**, *93*, 207–215. [[CrossRef](#)]
37. Carlsson, D.O.; Lindh, J.; Nyholm, L.; Strømme, M.; Mihranyan, A. Cooxidant-free TEMPO-mediated oxidation of highly crystalline nanocellulose in water. *RSC Adv.* **2014**, *4*, 52289–52298. [[CrossRef](#)]
38. Henriksson, M.; Henriksson, G.; Berglund, L.; Lindström, T. An environmentally friendly method for enzyme-assisted preparation of microfibrillated cellulose (MFC) nanofibers. *Eur. Polym. J.* **2007**, *43*, 3434–3441. [[CrossRef](#)]
39. Mokhena, T.C.; John, M.J. Cellulose nanomaterials: New generation materials for solving global issues. *Cellulose* **2020**, *27*, 1149–1194. [[CrossRef](#)]

40. Habibi, Y.; Dufresne, A. Highly filled bionanocomposites from functionalized polysaccharide nanocrystals. *Biomacromolecules* **2008**, *9*, 1974–1980. [[CrossRef](#)]
41. Zhao, J.; Wu, X.; Yuan, X.; Yang, X.; Guo, H.; Yao, W.; Ji, D.; Li, X.; Zhang, L. Nanocellulose and Cellulose Making with Bio-Enzymes from Different Particle Sizes of Neosinocalamus Affinis. *Coatings* **2022**, *12*, 1734. [[CrossRef](#)]
42. Fan, X.-M.; Yu, H.-Y.; Wang, D.-C.; Mao, Z.-H.; Yao, J.; Tam, K.C. Facile and green synthesis of carboxylated cellulose nanocrystals as efficient adsorbents in wastewater treatments. *ACS Sustain. Chem. Eng.* **2019**, *7*, 18067–18075. [[CrossRef](#)]
43. Wu, X.; Yuan, X.; Zhao, J.; Ji, D.; Guo, H.; Yao, W.; Li, X.; Zhang, L. Study on the effects of different pectinase/cellulase ratios and pretreatment times on the preparation of nanocellulose by ultrasound-assisted bio-enzyme heat treatment. *RSC Adv.* **2023**, *13*, 5149–5157. [[CrossRef](#)] [[PubMed](#)]
44. Rana, A.K.; Frollini, E.; Thakur, V.K. Cellulose nanocrystals: Pretreatments, preparation strategies, and surface functionalization. *Int. J. Biol. Macromol.* **2021**, *182*, 1554–1581. [[CrossRef](#)] [[PubMed](#)]
45. Li, J.; Zhang, F.; Zhong, Y.; Zhao, Y.; Gao, P.; Tian, F.; Zhang, X.; Zhou, R.; Cullen, P.J. Emerging Food Packaging Applications of Cellulose Nanocomposites: A Review. *Polymers* **2022**, *14*, 4025. [[CrossRef](#)]
46. Kargupta, W.; Seifert, R.; Martinez, M.; Olson, J.; Tanner, J.; Batchelor, W. Sustainable production process of mechanically prepared nanocellulose from hardwood and softwood: A comparative investigation of refining energy consumption at laboratory and pilot scale. *Ind. Crops Prod.* **2021**, *171*, 113868. [[CrossRef](#)]
47. Ellebracht, N.C.; Jones, C.W. Amine functionalization of cellulose nanocrystals for acid–base organocatalysis: Surface chemistry, cross-linking, and solvent effects. *Cellulose* **2018**, *25*, 6495–6512. [[CrossRef](#)]
48. Yeasmin, M.S.; Mondal, M.I.H. Synthesis of highly substituted carboxymethyl cellulose depending on cellulose particle size. *Int. J. Biol. Macromol.* **2015**, *80*, 725–731. [[CrossRef](#)]
49. Patoary, M.K.; Farooq, A.; Zaarour, B.; Liu, L. Phosphorylated cellulose nanofibrils: Structure-morphology-rheology relationships. *Cellulose* **2021**, *28*, 4105–4117. [[CrossRef](#)]
50. Duan, L.; Liu, R.; Duan, Y.; Li, Z.; Li, Q. A simultaneous strategy for the preparation of acetylation modified cellulose nanofiber/polypropylene composites. *Carbohydr. Polym.* **2022**, *277*, 118744. [[CrossRef](#)]
51. Okada, K.; Saito, Y.; Akiyoshi, M.; Endo, T.; Matsunaga, T. Preparation and characterization of nitrocellulose nanofiber. *Propellants Explos. Pyrotech.* **2021**, *46*, 962–968. [[CrossRef](#)]
52. Henschen, J.; Li, D.; Ek, M. Preparation of cellulose nanomaterials via cellulose oxalates. *Carbohydr. Polym.* **2019**, *213*, 208–216. [[CrossRef](#)]
53. Zhang, Y.; Chen, J.; Zhang, L.; Zhan, P.; Liu, N.; Wu, Z. Preparation of nanocellulose from steam exploded poplar wood by enzymolysis assisted sonication. *Mater. Res. Express* **2020**, *7*, 035010. [[CrossRef](#)]
54. Tao, P.; Wu, Z.; Xing, C.; Zhang, Q.; Wei, Z.; Nie, S. Effect of enzymatic treatment on the thermal stability of cellulose nanofibrils. *Cellulose* **2019**, *26*, 7717–7725. [[CrossRef](#)]
55. Nie, S.; Zhang, K.; Lin, X.; Zhang, C.; Yan, D.; Liang, H.; Wang, S. Enzymatic pretreatment for the improvement of dispersion and film properties of cellulose nanofibrils. *Carbohydr. Polym.* **2018**, *181*, 1136–1142. [[CrossRef](#)] [[PubMed](#)]
56. Kassab, Z.; Syafri, E.; Tamraoui, Y.; Hannache, H.; El Achaby, M. Characteristics of sulfated and carboxylated cellulose nanocrystals extracted from Juncus plant stems. *Int. J. Biol. Macromol.* **2020**, *154*, 1419–1425. [[CrossRef](#)]
57. Rasheed, M.; Jawaid, M.; Parveez, B.; Zuriyati, A.; Khan, A. Morphological, chemical and thermal analysis of cellulose nanocrystals extracted from bamboo fibre. *Int. J. Biol. Macromol.* **2020**, *160*, 183–191. [[CrossRef](#)]
58. Gatenholm, P.; Klemm, D. Bacterial nanocellulose as a renewable material for biomedical applications. *MRS Bull.* **2010**, *35*, 208–213. [[CrossRef](#)]
59. Stevanic, J.S.; Joly, C.; Mikkonen, K.S.; Pirkkalainen, K.; Serimaa, R.; Rémond, C.; Toriz, G.; Gatenholm, P.; Tenkanen, M.; Salmén, L. Bacterial nanocellulose-reinforced arabinoxylan films. *J. Appl. Polym. Sci.* **2011**, *122*, 1030–1039. [[CrossRef](#)]
60. Salari, M.; Khiabani, M.S.; Mokarram, R.R.; Ghanbarzadeh, B.; Kafil, H.S. Preparation and characterization of cellulose nanocrystals from bacterial cellulose produced in sugar beet molasses and cheese whey media. *Int. J. Biol. Macromol.* **2019**, *122*, 280–288. [[CrossRef](#)]
61. Xu, S.; Xu, S.; Ge, X.; Tan, L.; Liu, T. Low-cost and highly efficient production of bacterial cellulose from sweet potato residues: Optimization, characterization, and application. *Int. J. Biol. Macromol.* **2022**, *196*, 172–179. [[CrossRef](#)] [[PubMed](#)]
62. Liu, H.; Geng, B.; Chen, Y.; Wang, H. Review on the aerogel-type oil sorbents derived from nanocellulose. *ACS Sustain. Chem. Eng.* **2017**, *5*, 49–66. [[CrossRef](#)]
63. Long, L.-Y.; Weng, Y.-X.; Wang, Y.-Z. Cellulose aerogels: Synthesis, applications, and prospects. *Polymers* **2018**, *10*, 623. [[CrossRef](#)]
64. Li, K.; Chen, X.; Wang, Y.; Sun, B.; Yuan, Z.; Liu, Y. Regenerated cellulose microgel: A promising reinforcing agent and gelator for soft matter. *ACS Appl. Polym. Mater.* **2021**, *3*, 4101–4108. [[CrossRef](#)]
65. Xing, H.; Fei, Y.; Cheng, J.; Wang, C.; Zhang, J.; Niu, C.; Fu, Q.; Cheng, J.; Lu, L. Green Preparation of Durian Rind-Based Cellulose Nanofiber and Its Application in Aerogel. *Molecules* **2022**, *27*, 6507. [[CrossRef](#)] [[PubMed](#)]
66. Shaheed, N.; Javanshir, S.; Esmkhani, M.; Dekamin, M.G.; Naimi-Jamal, M.R. Synthesis of nanocellulose aerogels and Cu-BTC/nanocellulose aerogel composites for adsorption of organic dyes and heavy metal ions. *Sci. Rep.* **2021**, *11*, 18553. [[CrossRef](#)]
67. Heath, L.; Thielemans, W. Cellulose nanowhisker aerogels. *Green Chem.* **2010**, *12*, 1448–1453. [[CrossRef](#)]
68. Zhu, W.; Zhang, Y.; Wang, X.; Wu, Y.; Han, M.; You, J.; Jia, C.; Kim, J. Aerogel nanoarchitectonics based on cellulose nanocrystals and nanofibers from eucalyptus pulp: Preparation and comparative study. *Cellulose* **2022**, *29*, 817–833. [[CrossRef](#)]

69. Gupta, P.; Sathwane, M.; Chhajed, M.; Verma, C.; Grohens, Y.; Seantier, B.; Agrawal, A.K.; Maji, P.K. Surfactant Assisted In Situ Synthesis of Nanofibrillated Cellulose/Polymethylsilsesquioxane Aerogel for Tuning Its Thermal Performance. *Macromol. Rapid Commun.* **2023**, *44*, 2200628. [CrossRef]
70. Wu, Z.Y.; Liang, H.W.; Hu, B.C.; Yu, S.H. Emerging carbon-nanofiber aerogels: Chemosynthesis versus biosynthesis. *Angew. Chem. Int. Ed.* **2018**, *57*, 15646–15662. [CrossRef]
71. Shen, X.; Shamshina, J.L.; Berton, P.; Gurau, G.; Rogers, R.D. Hydrogels based on cellulose and chitin: Fabrication, properties, and applications. *Green Chem.* **2016**, *18*, 53–75. [CrossRef]
72. Mu, M.; Li, Y.; Yu, H.-Y.; Li, Z.; Cao, Y.; Chen, X. Construction of nanocellulose aerogels with mechanical flexibility and pH-responsive properties via a cross-linker structure design strategy. *ACS Sustain. Chem. Eng.* **2021**, *9*, 9951–9960. [CrossRef]
73. Ruan, J.-Q.; Xie, K.-Y.; Li, Z.; Zuo, X.; Guo, W.; Chen, Q.-Y.; Li, H.; Fei, C.; Lu, M.-H. Multifunctional ultralight nanocellulose aerogels as excellent broadband acoustic absorption materials. *J. Mater. Sci.* **2023**, *58*, 971–982. [CrossRef]
74. Surapolchai, W.; Schiraldi, D.A. The effects of physical and chemical interactions in the formation of cellulose aerogels. *Polym. Bull.* **2010**, *65*, 951–960. [CrossRef]
75. Li, Y.; Grishkewich, N.; Liu, L.; Wang, C.; Tam, K.C.; Liu, S.; Mao, Z.; Sui, X. Construction of functional cellulose aerogels via atmospheric drying chemically cross-linked and solvent exchanged cellulose nanofibrils. *Chem. Eng. J.* **2019**, *366*, 531–538. [CrossRef]
76. Wu, D.; Lv, P.; Feng, Q.; Jiang, Y.; Yang, H.; Alfred, M.; Wei, Q. Biomass-derived nanocellulose aerogel enable highly efficient immobilization of laccase for the degradation of organic pollutants. *Bioresour. Technol.* **2022**, *356*, 127311. [CrossRef]
77. Zhang, T.; Zhang, W.; Zhang, Y.; Shen, M.; Zhang, J. Gas phase synthesis of aminated nanocellulose aerogel for carbon dioxide adsorption. *Cellulose* **2020**, *27*, 2953–2958. [CrossRef]
78. Ciftci, D.; Ubeyitogullari, A.; Huerta, R.R.; Ciftci, O.N.; Flores, R.A.; Saldaña, M.D. Lupin hull cellulose nanofiber aerogel preparation by supercritical CO₂ and freeze drying. *J. Supercrit. Fluids* **2017**, *127*, 137–145. [CrossRef]
79. Li, J.; Tan, S.; Xu, Z. Anisotropic nanocellulose aerogel loaded with modified uio-66 as efficient adsorbent for heavy metal ions removal. *Nanomaterials* **2020**, *10*, 1114. [CrossRef]
80. Wu, Y.; Sun, M.; Wu, X.; Shi, T.; Chen, H.; Wang, H. Preparation of nanocellulose aerogel from the poplar (*Populus tomentosa*) catkin fiber. *Forests* **2019**, *10*, 749. [CrossRef]
81. Qiu, J.; Guo, X.; Lei, W.; Ding, R.; Zhang, Y.; Yang, H. Facile Preparation of Cellulose Aerogels with Controllable Pore Structure. *Nanomaterials* **2023**, *13*, 613. [CrossRef]
82. Wang, X.; Zhang, Y.; Jiang, H.; Song, Y.; Zhou, Z.; Zhao, H. Tert-butyl alcohol used to fabricate nano-cellulose aerogels via freeze-drying technology. *Mater. Res. Express* **2017**, *4*, 065006. [CrossRef]
83. Yang, X.; Cranston, E.D. Chemically cross-linked cellulose nanocrystal aerogels with shape recovery and superabsorbent properties. *Chem. Mater.* **2014**, *26*, 6016–6025. [CrossRef]
84. Wang, X.; Zhang, Y.; Jiang, H.; Song, Y.; Zhou, Z.; Zhao, H. Fabrication and characterization of nano-cellulose aerogels via supercritical CO₂ drying technology. *Mater. Lett.* **2016**, *183*, 179–182. [CrossRef]
85. Fu, J.; Wang, S.; He, C.; Lu, Z.; Huang, J.; Chen, Z. Facilitated fabrication of high strength silica aerogels using cellulose nanofibrils as scaffold. *Carbohydr. Polym.* **2016**, *147*, 89–96. [CrossRef]
86. Li, Y.; Tanna, V.A.; Zhou, Y.; Winter, H.H.; Watkins, J.J.; Carter, K.R. Nanocellulose aerogels inspired by frozen tofu. *ACS Sustain. Chem. Eng.* **2017**, *5*, 6387–6391. [CrossRef]
87. Zhang, X.; Liu, P.; Duan, Y.; Jiang, M.; Zhang, J. Graphene/cellulose nanocrystals hybrid aerogel with tunable mechanical strength and hydrophilicity fabricated by ambient pressure drying technique. *RSC Adv.* **2017**, *7*, 16467–16473. [CrossRef]
88. Pour, G.; Beauger, C.; Rigacci, A.; Budtova, T. Xerocellulose: Lightweight, porous and hydrophobic cellulose prepared via ambient drying. *J. Mater. Sci.* **2015**, *50*, 4526–4535. [CrossRef]
89. Zhao, S.; Malfait, W.J.; Guerrero-Alburquerque, N.; Koebel, M.M.; Nyström, G. Biopolymer aerogels and foams: Chemistry, properties, and applications. *Angew. Chem. Int. Ed.* **2018**, *57*, 7580–7608. [CrossRef]
90. Abdul Khalil, H.; Adnan, A.; Yahya, E.B.; Olaiya, N.; Safrida, S.; Hossain, M.S.; Balakrishnan, V.; Gopakumar, D.A.; Abdullah, C.; Oyekanmi, A. A review on plant cellulose nanofibre-based aerogels for biomedical applications. *Polymers* **2020**, *12*, 1759. [CrossRef]
91. Zhu, F. Starch based aerogels: Production, properties and applications. *Trends Food Sci. Technol.* **2019**, *89*, 1–10. [CrossRef]
92. Shi, W.; Ching, Y.C.; Chuah, C.H. Preparation of aerogel beads and microspheres based on chitosan and cellulose for drug delivery: A review. *Int. J. Biol. Macromol.* **2021**, *170*, 751–767. [CrossRef] [PubMed]
93. Rigueto, C.V.T.; Nazari, M.T.; Massuda, L.Á.; Ostwald, B.E.P.; Piccin, J.S.; Dettmer, A. Production and environmental applications of gelatin-based composite adsorbents for contaminants removal: A review. *Environ. Chem. Lett.* **2021**, *19*, 2465–2486. [CrossRef]
94. Alguacil, F.J.; López, F.A. Organic dyes versus adsorption processing. *Molecules* **2021**, *26*, 5440. [CrossRef] [PubMed]
95. Lan, D.; Zhu, H.; Zhang, J.; Li, S.; Chen, Q.; Wang, C.; Wu, T.; Xu, M. Adsorptive removal of organic dyes via porous materials for wastewater treatment in recent decades: A review on species, mechanisms and perspectives. *Chemosphere* **2021**, *293*, 133464. [CrossRef]
96. Wang, S.; Zhang, Q.; Wang, Z.; Pu, J. Facile fabrication of an effective nanocellulose-based aerogel and removal of methylene blue from aqueous system. *J. Water Process Eng.* **2020**, *37*, 101511. [CrossRef]
97. Xie, Q.; Zou, Y.; Wang, Y.; Wang, H.; Du, Z.; Cheng, X. Mechanically robust sodium alginate/cellulose nanofibers/polyethyleneimine composite aerogel for effective removal of hexavalent chromium and anionic dyes. *Polym. Eng. Sci.* **2022**, *62*, 1927–1940. [CrossRef]

98. Yu, Z.; Hu, C.; Dichiaro, A.B.; Jiang, W.; Gu, J. Cellulose nanofibril/carbon nanomaterial hybrid aerogels for adsorption removal of cationic and anionic organic dyes. *Nanomaterials* **2020**, *10*, 169. [[CrossRef](#)]
99. Maatar, W.; Boufi, S. Microporous cationic nanofibrillar cellulose aerogel as promising adsorbent of acid dyes. *Cellulose* **2017**, *24*, 1001–1015. [[CrossRef](#)]
100. Huo, Y.; Liu, Y.; Yang, J.; Du, H.; Qin, C.; Liu, H. Polydopamine-modified cellulose nanofibril composite aerogel: An effective dye adsorbent. *Langmuir* **2022**, *38*, 4164–4174. [[CrossRef](#)]
101. Grishkewich, N.; Li, Y.; Liu, K.; Tam, K.C. Synthesis and characterization of modified cellulose nanofibril organosilica aerogels for the removal of anionic dye. *J. Polym. Res.* **2022**, *29*, 261. [[CrossRef](#)]
102. Yi, X.; Wang, F.; Wu, Y.; He, J.; Huang, Y. Aramid nanofibers/bacterial cellulose nanocomposite aerogels for high-efficient cationic dye removal. *Mater. Chem. Phys.* **2021**, *272*, 124985. [[CrossRef](#)]
103. Nia, M.H.; Tavakolian, M.; Kiasat, A.R.; van de Ven, T.G. Hybrid aerogel nanocomposite of dendritic colloidal silica and hairy nanocellulose: An effective dye adsorbent. *Langmuir* **2020**, *36*, 11963–11974. [[CrossRef](#)]
104. Jiang, F.; Dinh, D.M.; Hsieh, Y.-L. Adsorption and desorption of cationic malachite green dye on cellulose nanofibril aerogels. *Carbohydr. Polym.* **2017**, *173*, 286–294. [[CrossRef](#)]
105. Yang, L.; Zhan, Y.; Gong, Y.; Ren, E.; Lan, J.; Guo, R.; Yan, B.; Chen, S.; Lin, S. Development of eco-friendly CO₂-responsive cellulose nanofibril aerogels as “green” adsorbents for anionic dyes removal. *J. Hazard. Mater.* **2021**, *405*, 124194. [[CrossRef](#)] [[PubMed](#)]
106. Du, N.; Huang, L.-Y.; Xiong, Y.-S.; Tian, R.; Yin, J.-Y.; Cao, D.-Y.; Hu, D.-B.; Lu, H.-Q.; Li, W.; Li, K. Micro-mechanism insights into the adsorption of anionic dyes using quaternary ammonium-functionalised chitosan aerogels. *Carbohydr. Polym.* **2023**, *313*, 120855. [[CrossRef](#)]
107. Kuang, J.; Cai, T.; Dai, J.; Yao, L.; Liu, F.; Liu, Y.; Shu, J.; Fan, J.; Peng, H. High strength chitin/chitosan-based aerogel with 3D hierarchically macro-meso-microporous structure for high-efficiency adsorption of Cu (II) ions and Congo red. *Int. J. Biol. Macromol.* **2023**, *230*, 123238. [[CrossRef](#)]
108. Zhang, Y.; Zhao, S.; Mu, M.; Wang, L.; Fan, Y.; Liu, X. Eco-friendly ferrocene-functionalized chitosan aerogel for efficient dye degradation and phosphate adsorption from wastewater. *Chem. Eng. J.* **2022**, *439*, 135605. [[CrossRef](#)]
109. Niu, C.; Zhang, N.; Hu, C.; Zhang, C.; Zhang, H.; Xing, Y. Preparation of a novel citric acid-crosslinked Zn-MOF/chitosan composite and application in adsorption of chromium (VI) and methyl orange from aqueous solution. *Carbohydr. Polym.* **2021**, *258*, 117644. [[CrossRef](#)] [[PubMed](#)]
110. Zhang, N.; Zang, G.-L.; Shi, C.; Yu, H.-Q.; Sheng, G.-P. A novel adsorbent TEMPO-mediated oxidized cellulose nanofibrils modified with PEI: Preparation, characterization, and application for Cu (II) removal. *J. Hazard. Mater.* **2016**, *316*, 11–18. [[CrossRef](#)]
111. Fei, Y.; Hu, Y.H. Design, synthesis, and performance of adsorbents for heavy metal removal from wastewater: A review. *J. Mater. Chem. A* **2022**, *10*, 1047–1085. [[CrossRef](#)]
112. Cao, C.-Y.; Cui, Z.-M.; Chen, C.-Q.; Song, W.-G.; Cai, W. Ceria hollow nanospheres produced by a template-free microwave-assisted hydrothermal method for heavy metal ion removal and catalysis. *J. Phys. Chem. C* **2010**, *114*, 9865–9870. [[CrossRef](#)]
113. Zito, P.; Shipley, H.J. Inorganic nano-adsorbents for the removal of heavy metals and arsenic: A review. *RSC Adv.* **2015**, *5*, 29885–29907. [[CrossRef](#)]
114. Chakraborty, R.; Asthana, A.; Singh, A.K.; Jain, B.; Susan, A.B.H. Adsorption of heavy metal ions by various low-cost adsorbents: A review. *Int. J. Environ. Anal. Chem.* **2022**, *102*, 342–379. [[CrossRef](#)]
115. Lam, B.; Déon, S.; Morin-Crini, N.; Crini, G.; Fievet, P. Polymer-enhanced ultrafiltration for heavy metal removal: Influence of chitosan and carboxymethyl cellulose on filtration performances. *J. Clean. Prod.* **2018**, *171*, 927–933. [[CrossRef](#)]
116. Geng, B.; Xu, Z.; Liang, P.; Zhang, J.; Christie, P.; Liu, H.; Wu, S.; Liu, X. Three-dimensional macroscopic aminosilylated nanocellulose aerogels as sustainable bio-adsorbents for the effective removal of heavy metal ions. *Int. J. Biol. Macromol.* **2021**, *190*, 170–177. [[CrossRef](#)]
117. Mo, L.; Zhang, S.; Qi, F.; Huang, A. Highly stable cellulose nanofiber/polyacrylamide aerogel via in-situ physical/chemical double crosslinking for highly efficient Cu (II) ions removal. *Int. J. Biol. Macromol.* **2022**, *209*, 1922–1932. [[CrossRef](#)]
118. Wang, M.; Shao, L.; Jia, M. Shape memory and underwater superelastic mof@ cellulose aerogels for rapid and large-capacity adsorption of metal ions. *Cellulose* **2022**, *29*, 8243–8254. [[CrossRef](#)]
119. Li, J.; Zuo, K.; Wu, W.; Xu, Z.; Yi, Y.; Jing, Y.; Dai, H.; Fang, G. Shape memory aerogels from nanocellulose and polyethyleneimine as a novel adsorbent for removal of Cu (II) and Pb (II). *Carbohydr. Polym.* **2018**, *196*, 376–384. [[CrossRef](#)]
120. Guo, D.-M.; An, Q.-D.; Xiao, Z.-Y.; Zhai, S.-R.; Shi, Z. Polyethylenimine-functionalized cellulose aerogel beads for efficient dynamic removal of chromium (VI) from aqueous solution. *RSC Adv.* **2017**, *7*, 54039–54052. [[CrossRef](#)]
121. Hong, H.-J.; Ban, G.; Kim, H.S.; Jeong, H.S.; Park, M.S. Fabrication of cylindrical 3D cellulose nanofibril (CNF) aerogel for continuous removal of copper (Cu²⁺) from wastewater. *Chemosphere* **2021**, *278*, 130288. [[CrossRef](#)] [[PubMed](#)]
122. Wei, J.; Yang, Z.; Sun, Y.; Wang, C.; Fan, J.; Kang, G.; Zhang, R.; Dong, X.; Li, Y. Nanocellulose-based magnetic hybrid aerogel for adsorption of heavy metal ions from water. *J. Mater. Sci.* **2019**, *54*, 6709–6718. [[CrossRef](#)]
123. Lei, C.; Gao, J.; Ren, W.; Xie, Y.; Abdalkarim, S.Y.H.; Wang, S.; Ni, Q.; Yao, J. Fabrication of metal-organic frameworks@ cellulose aerogels composite materials for removal of heavy metal ions in water. *Carbohydr. Polym.* **2019**, *205*, 35–41. [[CrossRef](#)]
124. Wang, Y.; Li, Y.; Zhang, Y.; Zhang, Z.; Li, Y.; Li, W. Nanocellulose aerogel for highly efficient adsorption of uranium (VI) from aqueous solution. *Carbohydr. Polym.* **2021**, *267*, 118233. [[CrossRef](#)]

125. Li, M.; Tang, C.; Fu, S.; Tam, K.C.; Zong, Y. Cellulose-based aerogel beads for efficient adsorption-reduction-sequestration of Cr (VI). *Int. J. Biol. Macromol.* **2022**, *216*, 860–870. [[CrossRef](#)]
126. Shahnaz, T.; Sharma, V.; Subbiah, S.; Narayanasamy, S. Multivariate optimisation of Cr (VI), Co (III) and Cu (II) adsorption onto nanobentonite incorporated nanocellulose/chitosan aerogel using response surface methodology. *J. Water Process Eng.* **2020**, *36*, 101283. [[CrossRef](#)]
127. Wang, Q.; Tian, Y.; Kong, L.; Zhang, J.; Zuo, W.; Li, Y.; Cai, G. A novel 3D superelastic polyethyleneimine functionalized chitosan aerogels for selective removal of Cr (VI) from aqueous solution: Performance and mechanisms. *Chem. Eng. J.* **2021**, *425*, 131722. [[CrossRef](#)]
128. Ghiorghita, C.-A.; Lazar, M.M.; Platon, I.-V.; Humelnicu, D.; Doroftei, F.; Dinu, M.V. Feather-weight cryostructured thiourea-chitosan aerogels for highly efficient removal of heavy metal ions and bacterial pathogens. *Int. J. Biol. Macromol.* **2023**, *235*, 123910. [[CrossRef](#)] [[PubMed](#)]
129. Li, Z.; Shao, L.; Ruan, Z.; Hu, W.; Lu, L.; Chen, Y. Converting untreated waste office paper and chitosan into aerogel adsorbent for the removal of heavy metal ions. *Carbohydr. Polym.* **2018**, *193*, 221–227. [[CrossRef](#)]
130. Li, S.; Li, Y.; Fu, Z.; Lu, L.; Cheng, J.; Fei, Y. A ‘top modification’ strategy for enhancing the ability of a chitosan aerogel to efficiently capture heavy metal ions. *J. Colloid Interface Sci.* **2021**, *594*, 141–149. [[CrossRef](#)]
131. Ye, X.; Shang, S.; Zhao, Y.; Cui, S.; Zhong, Y.; Huang, L. Ultra-efficient adsorption of copper ions in chitosan–montmorillonite composite aerogel at wastewater treatment. *Cellulose* **2021**, *28*, 7201–7212. [[CrossRef](#)]
132. Eniola, J.O.; Kumar, R.; Barakat, M.A. Adsorptive removal of antibiotics from water over natural and modified adsorbents. *Environ. Sci. Pollut. Res.* **2019**, *26*, 34775–34788. [[CrossRef](#)]
133. Yang, Y.; Song, W.; Lin, H.; Wang, W.; Du, L.; Xing, W. Antibiotics and antibiotic resistance genes in global lakes: A review and meta-analysis. *Environ. Int.* **2018**, *116*, 60–73. [[CrossRef](#)]
134. Li, S.; Zhang, Y.; You, Q.; Wang, Q.; Liao, G.; Wang, D. Highly efficient removal of antibiotics and dyes from water by the modified carbon nanofibers composites with abundant mesoporous structure. *Colloids Surf., A* **2018**, *558*, 392–401. [[CrossRef](#)]
135. Yao, Q.; Fan, B.; Xiong, Y.; Jin, C.; Sun, Q.; Sheng, C. 3D assembly based on 2D structure of cellulose nanofibril/graphene oxide hybrid aerogel for adsorptive removal of antibiotics in water. *Sci. Rep.* **2017**, *7*, 45914. [[CrossRef](#)]
136. Wang, J.; Yao, Q.; Sheng, C.; Jin, C.; Sun, Q. One-step preparation of graphene oxide/cellulose nanofibril hybrid aerogel for adsorptive removal of four kinds of antibiotics. *J. Nanomater.* **2017**, *2017*, 5150613. [[CrossRef](#)]
137. Wang, Z.; Song, L.; Wang, Y.; Zhang, X.-F.; Yao, J. Construction of a hybrid graphene oxide/nanofibrillated cellulose aerogel used for the efficient removal of methylene blue and tetracycline. *J. Phys. Chem. Solids* **2021**, *150*, 109839. [[CrossRef](#)]
138. Wei, M.; Zheng, H.; Zeng, T.; Yang, J.; Fang, X.; Zhang, C. Porous carbon aerogel derived from bacterial cellulose with prominent potential for efficient removal of antibiotics from the aquatic matrix. *Water Sci. Technol.* **2021**, *84*, 1896–1907. [[CrossRef](#)]
139. Liu, Q.; Yu, H.; Zeng, F.; Li, X.; Sun, J.; Hu, X.; Pan, Q.; Li, C.; Lin, H.; Min Su, Z. Polyaniline as interface layers promoting the in-situ growth of zeolite imidazole skeleton on regenerated cellulose aerogel for efficient removal of tetracycline. *J. Colloid Interface Sci.* **2020**, *579*, 119–127. [[CrossRef](#)]
140. Cui, F.; Li, H.; Chen, C.; Wang, Z.; Liu, X.; Jiang, G.; Cheng, T.; Bai, R.; Song, L. Cattail fibers as source of cellulose to prepare a novel type of composite aerogel adsorbent for the removal of enrofloxacin in wastewater. *Int. J. Biol. Macromol.* **2021**, *191*, 171–181. [[CrossRef](#)]
141. Ruan, C.; Chen, G.; Ma, Y.; Du, C.; He, C.; Liu, X.; Jin, X.; Chen, Q.; He, S.; Huang, Y. PVA-assisted CNCs/SiO₂ composite aerogel for efficient sorption of ciprofloxacin. *J. Colloid Interface Sci.* **2023**, *630*, 544–555. [[CrossRef](#)]
142. Zhao, L.; Dong, P.; Xie, J.; Li, J.; Wu, L.; Yang, S.-T.; Luo, J. Porous graphene oxide–chitosan aerogel for tetracycline removal. *Mater. Res. Express* **2013**, *1*, 015601. [[CrossRef](#)]
143. Li, L.; Li, Y.; Li, M.; Sun, Y.; Wang, H.; Cui, M.; Xu, W. Adsorption of tetracycline by *Nicandra physaloides* (L.) Gaertn seed gum and *Nicandra physaloides* (L.) Gaertn seed gum/Carboxymethyl chitosan aerogel. *Environ. Technol.* **2022**, *43*, 4237–4248. [[CrossRef](#)] [[PubMed](#)]
144. Ma, J.; Lei, Y.; Khan, M.A.; Wang, F.; Chu, Y.; Lei, W.; Xia, M.; Zhu, S. Adsorption properties, kinetics & thermodynamics of tetracycline on carboxymethyl-chitosan reformed montmorillonite. *Int. J. Biol. Macromol.* **2019**, *124*, 557–567.
145. Tao, T.; Li, G.; He, Y.; Duan, P. Hybrid carbon nanotubes/graphene/nickel fluffy spheres for fast magnetic separation and efficient removal of organic solvents from water. *Mater. Lett.* **2019**, *254*, 440–443. [[CrossRef](#)]
146. Motta, F.L.; Stoyanov, S.R.; Soares, J.B. Application of solidifiers for oil spill containment: A review. *Chemosphere* **2018**, *194*, 837–846. [[CrossRef](#)]
147. Angelova, D.; Uzunov, I.; Uzunova, S.; Gigova, A.; Minchev, L. Kinetics of oil and oil products adsorption by carbonized rice husks. *Chem. Eng. J.* **2011**, *172*, 306–311. [[CrossRef](#)]
148. Akhlamadi, G.; Goharshadi, E.K. Sustainable and superhydrophobic cellulose nanocrystal-based aerogel derived from waste tissue paper as a sorbent for efficient oil/water separation. *Process Saf. Environ. Prot.* **2021**, *154*, 155–167. [[CrossRef](#)]
149. Rosli, N.A.; Khairudin, F.A.; Kargarzadeh, H.; Othaman, R.; Ahmad, I. Hydrophobic-oleophilic gamma-irradiated modified cellulose nanocrystal/gelatin aerogel for oil absorption. *Int. J. Biol. Macromol.* **2022**, *219*, 213–223. [[CrossRef](#)]
150. Zhang, H.; Wang, J.; Xu, G.; Xu, Y.; Wang, F.; Shen, H. Ultralight, hydrophobic, sustainable, cost-effective and floating kapok/microfibrillated cellulose aerogels as speedy and recyclable oil superabsorbents. *J. Hazard. Mater.* **2021**, *406*, 124758. [[CrossRef](#)] [[PubMed](#)]

151. Wang, X.; Xie, Z.; Chen, Z.; Jiang, H. Hydrophobic and lipophilic cellulose nanocrystal aerogel prepared by methyltrichlorosilane via vapor-phase reaction. *J. Appl. Polym. Sci.* **2022**, *139*, e53045. [[CrossRef](#)]
152. Qiao, A.; Huang, R.; Penkova, A.; Qi, W.; He, Z.; Su, R. Superhydrophobic, elastic and anisotropic cellulose nanofiber aerogels for highly effective oil/water separation. *Sep. Purif. Technol.* **2022**, *295*, 121266. [[CrossRef](#)]
153. Mi, H.-Y.; Li, H.; Jing, X.; Zhang, Q.; Feng, P.-Y.; He, P.; Liu, Y. Superhydrophobic cellulose nanofibril/silica fiber/Fe₃O₄ nanocomposite aerogel for magnetically driven selective oil absorption. *Cellulose* **2020**, *27*, 8909–8922. [[CrossRef](#)]
154. Liu, Q.; Liu, Y.; Feng, Q.; Chen, C.; Xu, Z. Preparation of antifouling and highly hydrophobic cellulose nanofibers/alginate aerogels by bidirectional freeze-drying for water-oil separation in the ocean environment. *J. Hazard. Mater.* **2023**, *441*, 129965. [[CrossRef](#)]
155. Zhang, H.; Zhang, G.; Zhu, H.; Wang, F.; Xu, G.; Shen, H.; Wang, J. Multiscale kapok/cellulose aerogels for oil absorption: The study on structure and oil absorption properties. *Ind. Crops Prod.* **2021**, *171*, 113902. [[CrossRef](#)]
156. Gu, H.; Gao, C.; Zhou, X.; Du, A.; Naik, N.; Guo, Z. Nanocellulose nanocomposite aerogel towards efficient oil and organic solvent adsorption. *Adv. Compos. Hybrid Mater.* **2021**, *4*, 459–468. [[CrossRef](#)]
157. Wang, M.; Shao, C.; Zhou, S.; Yang, J.; Xu, F. Preparation of carbon aerogels from TEMPO-oxidized cellulose nanofibers for organic solvents absorption. *RSC Adv.* **2017**, *7*, 38220–38230. [[CrossRef](#)]
158. Ma, Z.; Han, Y.; Xing, X.; Zhu, H.; Wang, Q.; Wang, X. Preparation of micro-convex rough interface carbon aerogels with cellulose-lithium bromide (LiBr) molten salt hydrate gelled system and application of oil-water separation. *Colloids Surf. A* **2022**, *650*, 129624. [[CrossRef](#)]
159. Zhou, X.; Fu, Q.; Liu, H.; Gu, H.; Guo, Z. Solvent-free nanoalumina loaded nanocellulose aerogel for efficient oil and organic solvent adsorption. *J. Colloid Interface Sci.* **2021**, *581*, 299–306. [[CrossRef](#)]
160. Chhajed, M.; Verma, C.; Singh, S.; Maji, P.K. Synergistic effect of natural rubber for imparting hydrophobicity in nanocellulose aerogel through one-pot synthesis and its application in oil/organic solvent sorption. *J. Water Process Eng.* **2023**, *51*, 103471. [[CrossRef](#)]
161. Fan, B.; Qi, B.; Wang, P.; Liu, Y.; Yu, Y.; Wang, Q.; Ren, X. Mechanically Tough and Regenerable Antibacterial Nanofibrillated Cellulose-Based Aerogels for Oil/Water Separation. *Langmuir* **2022**, *38*, 10716–10727. [[CrossRef](#)] [[PubMed](#)]
162. Zhang, M.; Jiang, S.; Li, M.; Wang, N.; Liu, L.; Liu, L.; Ge, A. Superior stable, hydrophobic and multifunctional nanocellulose hybrid aerogel via rapid UV induced in-situ polymerization. *Carbohydr. Polym.* **2022**, *288*, 119370. [[CrossRef](#)] [[PubMed](#)]
163. Zhang, Y.; Yin, M.; Li, L.; Fan, B.; Liu, Y.; Li, R.; Ren, X.; Huang, T.-S.; Kim, I.S. Construction of aerogels based on nanocrystalline cellulose and chitosan for high efficient oil/water separation and water disinfection. *Carbohydr. Polym.* **2020**, *243*, 116461. [[CrossRef](#)] [[PubMed](#)]
164. Fan, S.; Li, Z.; Fan, C.; Chen, J.; Huang, H.; Chen, G.; Liu, S.; Zhou, H.; Liu, R.; Feng, Z. Fast-thermoreponsive carboxylated carbon nanotube/chitosan aerogels with switchable wettability for oil/water separation. *J. Hazard. Mater.* **2022**, *433*, 128808. [[CrossRef](#)]
165. Li, A.; Lin, R.; Lin, C.; He, B.; Zheng, T.; Lu, L.; Cao, Y. An environment-friendly and multi-functional absorbent from chitosan for organic pollutants and heavy metal ion. *Carbohydr. Polym.* **2016**, *148*, 272–280. [[CrossRef](#)] [[PubMed](#)]
166. Lu, H.; Jiang, X.; Wang, J.; Hu, R. Degradable composite aerogel with excellent water-absorption for trace water removal in oil and oil-in-water emulsion filtration. *Front. Mater.* **2022**, *9*, 1093164. [[CrossRef](#)]

Disclaimer/Publisher’s Note: The statements, opinions and data contained in all publications are solely those of the individual author(s) and contributor(s) and not of MDPI and/or the editor(s). MDPI and/or the editor(s) disclaim responsibility for any injury to people or property resulting from any ideas, methods, instructions or products referred to in the content.